User-oriented hydrological indices for early warning system. Validation using post-event surveys: flood case studies on the Central Apennines District.

Annalina Lombardi[1], Valentina Colaiuda[1,2], Marco Verdecchia[2] and Barbara Tomassetti[1]

[1]CETEMPS, Centre of Excellence University of L'Aquila, via Vetoio, 67100 Coppito (L'Aquila), Italy
[2]Department of Physical and Chemical Sciences, University of L'Aquila, via Vetoio, 67100 Coppito (L'Aquila) Italy

Correspondence to: Annalina Lombardi (annalina.lombardi@univaq.it)

Abstract. Floods and flash floods are complex events, depending on weather dynamics, basin physiographical characteristics, land use cover and water management. For this reason, prediction of such events usually deals with very accurate model tuning and validation, which is usually site-specific and based on climatological data, such as discharge time series or flood databases. In this work, we developed and tested two hydrological stress indices for flood detection in the Central Italy Apennine District: a heterogeneous geographical area, characterized by complex topography and medium-to-small catchment extension. Proposed indices are threshold-based and developed considering operational requirements of Civil Protection end-users. They are calibrated and tested through the application of signal theory, in order to overcome data scarcity over ungauged areas, as well as incomplete discharge time series. The validation has been carried out on a case study basis, using flood reports from various source of information, as well as hydrometric level time series, which represent the actual hydrological quantity monitored by civil protection operators. Obtained results shows that the overall accuracy of flood prediction is greater than 0.8, with false alarm rates below 0.5 and probability of detection ranging from 0.51 to 0.80. Moreover, the different nature of the proposed indices suggests their application in a complementary way, as the index based on drained precipitation appears to be more sensible to rapid flood propagation in small tributaries, while the discharge-based index is particularly responsive to main channel dynamics.

1 Introduction

Floods are recognized among the most destructive natural hazards (Berz et al., 2001), affecting 21 mln people, globally, each year; unfortunately, this dramatic estimation is expected to rise up to 54 mln by 2030 (Lehman, 2015). So far, according to the data reported by MunichRe (2018), 2017 is considered the worst year in terms of overall losses caused by natural hazards.
It has also been long recognized as the increase in the frequencies of severe precipitation events represents a characteristic signature of observed climate changes at global scale; the intensification of the hydrological cycle due to the warming climate is projected to change river floods magnitude and frequency (Field et al. 2012, Blöschl et al., 2017). Kundzewicz and Schellnhuber (2004) highlighted that about one-third of all reported events and one-third of economic losses resulting from

natural catastrophes are attributable to floods all over the world. Different works seek to analyse the impact of Climate Change Scenario on flood hazards in Europe, finding as several European countries will experience increasing flood risk in the future (Dankers and Feyen 2009; Feyen et al., 2012). Alfieri et al. (2015) showed a significant increase in the frequency of extreme events (i.e., larger than 100 %) in 21 out of 37 European countries, in the reference period 2006–2035, to be followed by a further deterioration in the subsequent future. Blöschl et al. (2019) demonstrated clear regional patterns of both increasing and decreasing river flood discharges in the past five decades in Europe, attributable to changing climate. More specifically, the Mediterranean area is one of the climate system's most responsive hotspot to climate changes (Giorgi, 2006; Giorgi and Lionello, 2008). Indeed, 185 flood events were recorded in the Mediterranean countries between 1990 and 2006, being the number of cases affecting Spain, Italy and France 59% of the total. In the Italian Peninsula, these events caused 20 billion of damages to buildings and infrastructures (Llasat et al., 2010). Mysiak et al. (2013) estimated about some 3.5 million people (6 % of the total Italian population) live in hydrogeological risk areas. History of Italy is characterized by many devastating floods, causing deaths, relevant economic losses and deep social and environmental impact. Given the high landscape variability, the complex topography and climatic variability, Italy is one of the most exposed countries to geomorphological risk. Meteorological patterns are frequently characterized by deep convective clouds, that originates intense and localized rainfall, rapidly developing in localized floods. Salvati et al. (2018) estimated that 441 flood events occurred over 420 Italian sites from 1965 to 2014, causing a total amount of 771 fatalities.

Considering the last two decades, Italy is the sixth country in the world for number of victims caused by hydrogeological hazards and eighteenth in terms of economic losses (Eckstein et al., 2019). The European Parliament defined floods as *"the potential to cause fatalities, displacement of people, and damage to the environment, which can severely compromise economic development"*.

In the EU Directive 2007/60/CE concerning the "Assessment and management of flood risks", the realization of a flood risk map is foreseen over river basins with a significant potential risk of flooding (European Parliament, 2007). To this aim, tools for flood events prediction may also provide useful information for the mitigation strategies during the planning phase. Since the 1970s, the hydrological forecast has improved (e.g., Jain et al., 2018; Ranit and Durge, 2018; Hapuarachchi et al., 2011); a comprehensive review of the different hydrological forecasting techniques is given in Teng (2017), where empirical models are found to be sufficiently suitable for post-event monitoring and analysis, while hydrodynamic models are better indicated for dams and flash floods assessment. Eventually, simplified conceptual models are applicable for probabilistic flood risk assessment and multi-scenario modelling in well-defined channels. The data availability for the validation of hydrological models also influences the choice of the most suitable forecasting system (Jain et al., 2018, Cloke and Peppenberger, 2008).

The use of deterministic hydrological models for a hydrological forecast involves a series of critical points. First of all, the need to calibrate and validate models with very long time series of flow discharge data. These data are not always available, in particular on small seasonal streams, usually not instrumented, but more prone to destructive flooding phenomena (Alfieri et al., 2017). Furthermore, there is significant uncertainty in river discharge estimations due to rating curve interpolation and extrapolation, the presence of unsteady flow conditions and the seasonal changes of the river roughness (Di Baldassarre and

Montanari, 2009; Di Baldassarre and Claps, 2011). Moreover, it is difficult to establish a flow discharge threshold value, beyond which the river can be considered under stress conditions; this value is site-specific and refers to a certain river section, therefore, cannot be considered as general for the whole drainage network.

In the IPCC SREX report (Field et al., 2012), floods are defined as: "*the overflowing of the normal confines of a stream or other body of water or the accumulation of water over areas that are not normally submerged. Floods include river (fluvial) floods, flash floods, urban floods, pluvial floods, sewer floods, coastal floods, and glacial lake outburst flood*". Precipitation intensity, duration, amount, and timing are the principal mechanisms affecting a flood event. Moreover, the relationship between the rainfall and drainage network response is complex (Bates et al., 2008; Kundzewicz et al., 2012) and sensible to rain spatial distribution. In large river basins, for example, river floods are generated by intense and enduring rain while short-duration, highly intense rainfall is expected to determine floods in small basins. Chen et al., 2010 have highlighted different flooding drivers. The main ones are: i) pluvial flood, due to the limited capacity of a drainage system and ii) fluvial flood, caused by deluges from the river channel. The fluvial flood events considerably differ from pluvial (rainfall) flood events in spatial-temporal scale including their magnitude. The fluvial events usually occur for the duration of days or even weeks with widespread damages in the floodplains of the river system. On the other hand, pluvial flooding hardly ever happens for more than one-day duration with an influence on local regions (Chen et al., 2010; Patra et al., 2016; Apel et al., 2016).

In general, precipitation indices are applied for flash floods prediction, since a negligible contribution of infiltration processes is assumed for small catchments (Reed et al., 2007; Hurford et al. 2012; Ahn and Il Choi, 2013). Moreover, Alfieri et al. (2012) highlighted as precipitation-based indices are preferable over uninstrumented rivers. Schroeder et al. (2016) developed a flash flood severity index, universally applicable to all geographic locations, but many other authors had obtained better prediction scores by using runoff thresholds indices (Norbiato et al., 2009; Javelle et al., 2010; Raynaud et al., 2015; Alfieri et al. 2014), where thresholds are chosen on a climatological basis, for a given return period. However, the application of such indices is limited to historically monitored river segments, where a reference climatology is available. When historical runoff estimations are not available, validation is carried out on a case-study basis, if a reference flood hydrograph is available at station level (Nikolopoulos et al., 2013; Silvestro et al., 2015). Eventually, for validations of hydrological models assimilating rainfall estimation from remote sensing techniques, the reference flood hydrograph is obtained by forcing the hydrological model with rain gauges observations (Borga, 2002; Vieux and Bedient, 2004; Berenguer et al., 2005).

Given the complexity of the topic, many authors have recognized as an effective design of Early Warning Systems (EWSs) is a key element for fostering forecast skills and improve the resilience to natural hazards (Basha and Rus, 2007; Alfieri et al., 2011; Alfieri et al., 2012; Kundzewicz, 2012; Krzhizhanovskaya et al., 2012; Mysiak et al., 2013; Corral et al., 2019). In this framework, scientists in different fields have to deal with an effective development of new robust techniques and analyses. On the other hand, the achieved results need to be useful for the end, matching specific requirements. Horlick-Jones (1995) was the first to highlight the necessity of structured collaboration between Civil Protection and scientists, in the framework of the United Nations International Decade of Natural Disaster Reduction. Italian Legislative decree 02/01/2018 n. 1 defines, in art. 19, the role of the scientific community participating in the National Civil Protection Service, whose task is the development

of products deriving from research and innovation activities aimed at managing emergencies and risk preventing and forecasting. This study results from the need to identify useful and easy-to-understand tools for flood events prediction.

In the proposed work, several flood events affecting the Italian peninsula in the last years have been analysed, to assess the possibility to define a general-purpose alarm index to highlight segments of drainage network where critical stresses are expected. The idea of hydrological stress index arose from the collaboration with Civil Protection; this method is currently used in the framework of the Agreement between the Centre of Excellence CETEMPS and the Abruzzo Regional Functional Centre, where the former was appointed as Competence Centre of the Italian Civil Protection and Abruzzo Region, as well. In detail, we developed and validated two hydrological stress indices, related to different flooding drivers over Central Italy. Due to its complex topography, Central Apennines District (Central Italy, Figure 1) is characterized by both large and structured catchments (e.g., Tiber and Aterno-Pescara, see next section) and short ephemeral tributaries and torrents, which have a faster response to weather extremes and are more likely to be hit by a flash flood. Little information is available for those small catchments and hydrometric/discharge thresholds are, hence, difficult to define. The discussed indices are meant to be used in a complementary way, having the advantage of being strongly user-oriented, as they are calibrated taking into account a correspondence between the issued Civil Protection alarm level and index threshold. The innovative nature of the presented hydrological stress indices lies in the definition of a unique index threshold, associated to an alarm state, which assumes the same value over each point of the drainage network reconstructed by the model. They have been conceived to be applied over an interregional domain, devoid of climatological hydro-meteorological time-series. Before evaluating the performance of the hydrological forecast through the use of these indices, a procedure for their validation on past floods is to be defined, by assimilating observed meteorological data. The proposed evaluation procedure is designed to tackle with hydrological data scarceness and takes advantage from the signal theory processing methods.

The paper is organized as follows: a detailed description of the chosen hydrological model and of the proposed hydrological stress indices is reported in section 2, while a detailed description of the validation methods is provided in section 3. In section 4 the geographical framework of the study area is described and in section 5 the application of the proposed approach to several case studies is discussed.

2 Cetemps Hydrological Model

The Cetemps Hydrological Model (CHyM, hereafter) has been developed at Centre of Excellence Cetemps, since 2002 (Verdecchia et al., 2008b, Coppola et al., 2007). The original purpose was the development of an operational hydrological model for flood alert mapping (Tomassetti et al., 2005). However, the CHyM model has also been applied for climatological studies to investigate the effects of Climate Changes on the hydrological cycle (Coppola et al., 2014, Sangelantoni et al., 2019). CHyM is a fully distributed, physical-based hydrological model, where main hydrological processes are explicitly simulated by a physical-based numerical scheme.

An important characteristic of the model is the possibility to simulate the hydrological cycle over any geographical domain with any spatial resolution up to the DEM resolution. To this aim, the NASA SRTM DEM source file (https://lpdaac.usgs.gov/products/srtmgl3v003/) is implemented in the model with a native resolution of 90 m. Therefore, the CHyM model can simulate geographical domains with horizontal resolutions ≥ 90 m, even if the lower limit in choosing the spatial resolution deals with the validity of the numerical schemes used to simulate the hydrological processes (e.g.: the kinematic wave of shallow water, which used to solve the continuity equation, is considered a good approximation with a horizontal resolution of few hundreds meters).

For our national operational activity, we had divided the Italian territory in 7 geographical sub-domains, each one characterized by a spatial resolution which is chosen in order to optimize computational requirements (lower resolutions means faster simulations) and the correct drainage network extraction (higher resolutions means more accurate drainage network reconstruction). In this paper, the operational spatial resolution associated to each sub-domain is the same of the operational set-up (Taraglio et al., 2019; Colaiuda et al., 2020). Starting from the NASA data, the DEM is upscaled by applying the Cellular Automata spatial interpolation technique (Coppola et al., 2007).

In this section, the surface runoff calculation scheme is described in details; other parameterizations, such as evapotranspiration, infiltration, melting and return flow, are described in Coppola et al. (2014).

2.1 Runoff

To simulate the surface runoff, the continuity equation for surface routing and channel flow is explicitly solved. The flow direction for each grid point is established following the minimum energy principle; therefore, the flow direction is assigned to the adjacent grid-point located to the maximum downhill slope. The channel flow is computed according to the kinematic wave approximation of the shallow water equation (Lighthill and Whitham, 1955), where the continuity equation is expressed through the following simplified form:

$$\frac{\partial Q}{\partial x} + \frac{\partial A}{\partial t} = q \tag{2.1.1}$$

where, A is the flow cross-sectional area, Q is the flow rate of water discharge (m^3/s); q is the rate of lateral water inflow per unit of length, t is the time and x is the coordinate along the river path.

According to the shallow water approximation, the De Saint-Venant equation for the momentum conservation is expressed through the rating curve approximation:

$$Q = \alpha A^m \tag{2.1.2}$$

where, α is the kinematic wave parameter, and *m* is the kinematic wave exponent, adimensional, which is assumed to be ≈ 1 for cylindrical river geometry. The kinematic wave parameter α has the dimension of a speed:

$$\alpha = \frac{S^{1/2} R^{2/3}}{n(\mu)} \tag{2.1.3}$$

where *S* is the longitudinal bed slope of the flow element, *n* is the Manning's roughness coefficient, depending on the land use type μ, *R* is the hydraulic radius, considered as a linear function of the drained area *D*, according to the following formula:

$$R = \beta + \gamma D^{\delta} \tag{2.1.4}$$

where β, γ, and δ are empirical constants to tune in the calibration phase. If the hydraulic radius is expressed in meters and the drained area is expressed in km^2, typical values of β, γ, and δ are 0.0015, 0.35, and 0.33, respectively.

As for the surface flow outside the channel network, we assume that the surface water depth *y* is constant over each grid-point, therefore, the continuity equation assumes the following form:

$$\frac{\partial \varphi}{\partial x} + \frac{\partial y}{\partial t} = \xi \tag{2.1.5}$$

where φ is flow rate over the longitudinal dimension (m^2/s) of the grid point and ξ is the rate of water inflow per unit of area (m/s). The momentum equation has a linear relationship between the flow rate and the water depth, but Manning's roughness coefficient is increased by a factor M_n as the water is assumed to flow with a lower speed. For the operational simulations, the model default value of M_n for a river grid point is set to 4.5, but this parameter can be established during the calibration phase. An arbitrary drained area threshold of 100 km^2 is set to distinguish the overland flow from the channel flow, which is expected to occur for drained areas wider than that threshold.

2.2 CHyM Flood stress indices for operational activities

The hydrological model, CHyM, has been widely calibrated using climatological discharge time series of the Po river, as reported in Coppola et al. (2014). To this aim, it is important to note that the conditions of the Po River are representative of many alluvial rivers in Europe (Di Baldassarre et al., 2009).

In general, long time series of flow discharge data are necessary to calibrate and validate hydrological models. However, such data are not always available from all Italian regions and, in many cases, rating curves used for the discharge estimation are not constantly updated. Furthermore, hydrometric level measurements are not or less available for major floods, when sensors

installed along rivers stops to work, due to severe meteorological conditions. For this reason, many data in the upper part of the rating curve are missed and larger errors in the discharge estimation are often associated to higher discharge bins. Finally, hydrometers are installed over main river channels and small catchments are often excluded from discharge estimations, even if they are more prone to destructive flooding phenomena, especially in a complex orography context. Hydrometric/discharge thresholds are defined punctually and differs for each sensor. In our stress indices approach, discharge and runoff are combined with geographical information related to the upstream basin displacement, using other variables, such as the hydraulic radius (a linear function of the drained area) and time of concentration (that implicitly consider runoff conditions upstream). Therefore, they are able to give information in each point of the drainage network and their mutual variation from upstream to downstream along the river path is proportional. For this reason, general thresholds, valid in all grid-points of the drainage network may be defined. Moving from discharge-only to combined discharge-based and runoff-based indices, with the aim of calibrating such indices on threshold-basis for flood alert purposes, gives us the possibility to calibrate and validate a different information, which is not the discharge amount, but the river stress conditions, that is given by Civil Protection Authorities using hydrometric thresholds, as well as stress timing. Furthermore, the good estimatation of the stress state on a river channel is also provided by event reports and from press releases in those locations where no sensors are installed and, hence, no threshold are defined. Since the indices validation is not numerical, the problem of missing discharge data is overcome, being the threshold-based calibration a sufficient condition for our purpose to validate an alert system, rather than physical quantities. Moreover, it is important to highlight the influences of various flooding drivers (Ashley et al., 2005; Balmforth et al., 2006) since pluvial flooding happens together with fluvial flooding. Those flood scenarios were derived, for example, by adding rainstorms to the fluvial flood events and this condition is easily found when we consider Italian river basins with a size even up to a few tens of km. In this case, fluvial and pluvial floods are combined and are sufficient from a few days to a few hours of intense rainfall, depending on the considered basin. For this reason, we developed two different indices linked to the different flooding sources: CHyM Alert Index (CAI), a pluvial flood index, related to the limited capacity of a drainage systems, and Best Discharge-based Drainage (BDD), a fluvial flood index, related to deluges from river channels. These indices and the associated stress thresholds are general; the signal of the hydrological forecast is easy and quick to understand.

The hydrological stress indices use the quantity of drained water and the geomorphological characteristics of the different basins. Although the units of measurement of the indices are expressed in mm, they do not represent rainfall. Both indices refer to the water accumulated on the ground over the time. Three different thresholds for each of the two indices have been defined, in accordance with the protocols in use at the National Civil Protection Department. Since our intention is to develop unique thresholds with the same values in all grid-points, we had to optimize threshold choice to maximize hit rate and minimize false alarms. In order to avoid some further burdening of this paper, only results related to the moderate threshold (orange, pre-alert) are reported. The reason of our preference on this threshold lays on the consideration of its meaning in the Civil Protection alert system. In fact, the orange threshold exceedance can be considered the most crucial one for the Civil Protection Organization, because its exceedance starts the activation of protection measures for people and infrastructure safety, as foreseen in risk plans. The indices have been tested over a wide area in Central Italy, where many different catchments

are located. Indices validation is presented in "perfect conditions" i.e., forcing the hydrological model with observed meteorological variables. In our operational activity, as stressed out in Ferretti et al. (2020) and Colaiuda et al. (2020), the CHyM model uses meteorological observed data for the spin-up process and meteorological model output to predict hydrological stress for the next 24/48 hours. Therefore, the indices stress map is released from 6 to 48 hours in advance in the operational set-up.

2.2.1 CHyM Alert Index

The CHyM Alert Index (CAI) has been long used for the operational activities of flood alert mapping in Central Italy. CAI is calculated as a function of the rainfall drained by each elementary cell of the simulated geographical domain. More specifically, the index is associated to each grid-point, being the ratio between the total drained precipitation and total drained area in the upstream basin, respect to the specific grid-point. The proposed definition of the hydrological stress index has also a simple physical interpretation: it represents the average precipitation drained by each cell, considering the rain falling over the whole upstream basin of the selected cell, during a time interval corresponding to the mean time of concentration. A first version of the CAI index is described and tested in Tomassetti et al. (2005) and Verdecchia et al. (2008a); in its initial formulation, the mean time of concentration of the upstream basin was considered as a fixed term (36 or 48 hours, depending on the basin dimension). An updated version is presented in this work, where the average time of concentration, t_c is explicitly calculated from each drainage path *k*, down to the considered grid-point of coordinate *i,j*

$$\overline{t_c^{i,j}} = \sum_{k=1}^{N} \frac{t_{k\to ij}^{i,j}}{N} \tag{2.2.1}$$

where *N* indicates the total possible flowing paths.

The time of concentration is computed for each grid-point of the geographical domain. It can be defined as the time required to a raindrop to travel from the hydraulically most distant point in the watershed to the outlet. The outlet must be intended in the numerical sense; namely, it may be a "mouth cell" draining toward a sea point, a "tributary mouth cell" draining toward the interception with the main river or a cell draining toward the border of the simulated domain. The water velocity for each cell of the domain is computed according to the equation [2.1.3]. The time of concentration used in the CAI calculation is an average calculated on all possible times of concentration resulting from draining paths toward the considered grid-point.

The updated formula of the CAI index is then the following:

$$CAI = \frac{\int_{UP} \int_{t-\Delta t}^{t} P(t,s)\,dt\,ds}{\int_{UP} ds} \tag{2.2.2}$$

being *P* the precipitation available for the runoff. The integral over the space *s* is calculated considering the whole upstream basin of the selected cell. For the stress state identification, three different thresholds have been defined, after carrying out empirical tests: each threshold has been adequately chosen to qualitatively match the three different Civil protection state of hydrological criticality, as defined by the Head of Civil Protection Department (2016):

1. Ordinary Stress: 30 mm/day.
2. Moderate Stress: 60 mm/day.
3. High Stress: 110 mm/day.

The definition of each hydrogeological criticality level (and related colour-codes) is summarized in Table 1.

2.2.2 Best Discharge-based Drainage index

The BDD index is linked to the CHyM predicted discharge and is calculated, for each grid-cell of the drainage network, according to the following formula:

$$BDD(t) = \frac{Q(t)}{R^2} \tag{2.2.3}$$

where *Q* is the discharge predicted at time *t* and *R* is the hydraulic radius of the selected elementary cell, calculated as a linear function of the upstream basin (see equation [2.1.4]). BDD stress thresholds have been chosen following the same approach used for the CAI thresholds, in order to match the three relevant hydrological criticality levels:

1. Ordinary Stress: 3 mm/h;
2. Moderate Stress: 6 mm/h;
3. High Stress: 11 mm/h.

3 Materials and methods

Floods are complex events and data collection is not an easy task to achieve in this matter. The Italian government introduced the "Cadastre of Events", in response to Directive 2000/60/CE, a registry where relevant hydro-meteorological events are listed and associated to a heterogeneous database of different territorial data, organised in geo-referred layers (e.g., flood time, localization and damages). Data sources are not necessarily objective measurements: collections may contain official Civil Protection reports and press releases, as well as other reports from local authorities. The official Hydrogeological Catastrophes GIS archive is available online at: http://sici.irpi.cnr.it. However, the database updating was concluded in 2000: after this date, only few Italian Regions had moved to an alternative way of data collection, mainly represented by regional databases with different data structure and classification, freely or restrictively accessible for external users. Considering the lack of official

updated databases in the studied area, a huge, but necessary, effort was carried out to collect all available territorial data for the selected case studies, following the approach of the "Cadastre of Events", in order to create an Own Data Base (ODB) with territorial, geo-referred information. Collected information in ODB were used as reference data for the indices validation process, discussed in the following section.

ODB was filled by searching and classifying the following heterogeneous data about the considered flood events:

- official Civil Protection Event Reports, issued by regional Functional Centres or environmental agencies;
- COPERNICUS Emergency Management Service;
- POLARIS database by CNR-IRPI;
- data from the AVI Project;
- press releases;
- photographic documentation from social media (e.g., YouTube, YouReporter, etc…), reporting major rainfall events, floods and landslides causing direct human consequences and damages in the investigated period;
- available hydrometric level time series and thresholds, where updated (from Dewetra Platform, Italian Civil Protection Department and CIMA Research Foundation, 2014).

The above listed information was not all available for the same case study (CS), for this reason, a summary of the found validation material for each event is reported in Table 2. Moreover, to provide an overview of the data collection geographical distribution, the same information listed in Table 2 have been geo-referred and shown in the map of Figures 2, 3 and 4. Besides the territorial information, other hydrological data were used for the validation process. The Italian Prime Minister Decree (DPCM) issued on 27 February 2004 and concerning the "Operating concepts for functional management of national and regional alert system during flooding and landslide events for Civil Protection activities purposes", establishes the Regional Functional Centres to acquire and collect real-time data from monitoring networks. Hydrometric levels are identified as the quantities to be monitored in order to assign the critical level for, at least, moderate and high hydraulic risk to each warning area, through the definition of thresholds. Article 5 of the same Decree define as the real-time validation of prediction systems is made through the monitoring of moderate and high hydrometric level thresholds exceedances, for the main river channels. Secondary drainage network with drained area less than 400 km^2 are not included in this kind of validation.

The definition of water level critical thresholds (Italian Laws no. 59/2004, Fassi et al. 2008), is carried out for each Italian Region by local Civil Protection Authorities (Regional Functional Centres) at station level (Fassi et al., 2008; Brandolini et al., 2012; Mysiak et al., 2013). A colour code is then assigned to each hydrometric threshold (see details in table 1), indicating four different alarm levels, corresponding to specific hydraulic risk management actions, activated at institutional level (Italian Legislative Decree no. 01/2018). However, as recognized by the Italian Institute for Environmental Protection and Research (ISPRA), the hydrometric level is a strongly non-stationary variable, as it is influenced by the riverbed erosion and deposition processes (Braca et al., 2013). The hydrometric zero needs to be recalibrated, establishing an updating frequency adequate for the river flow regime and local hydrogeological factors. Moreover, the calibration should be carried out after flood occurrences, when the riverbed shape is significantly modified. Then, the hydrometric thresholds need to be revised correspondingly. After

the application of the Italian Law no. 183/1989, the management of the gauge's network and data collection is devoted to the Regional authorities. Even though a territorial approach is useful for a rapid response to risk scenarios, competences fragmentation among different entities had caused inhomogeneities on hydro-meteorological data availability and quality (e.g. rating curve updates, historical hydro-meteorological data time series, hydrometric threshold availability for all stations, etc...) with significant differences among the twenty Italian regions.

For all the aforementioned reasons, a deterministic hydrological flood prediction validation over a wide, interregional area can be challenging or not universally applicable, due to missing or obsolete information. Moreover, the discharge computation in hydrological models is affected by systematic biases when the hydrological network is exploited for hydropower production, irrigation, or industrial and domestic usage: in most cases, data about water uptake are scanty or incomplete, as they are collected by a variety of public and private actors and difficult to obtain. Another common issue for the spatial validation deals with thresholds inference on ungauged areas. Alfieri et al. (2017) highlighted that floods and flash floods usually occur in ungauged catchments: for those situations, post-event survey reports represent the only source of information. Besides, even if present, gauges data may be unavailable during a severe event or damaged by the flood.

The hydrological stress indices validation was first assessed through a qualitative approach, by selecting the strongest recorded signal of upcoming severe events from the hydrometric level time series and verifying the actual occurrence of floods in the areas where they were forecasted. To this aim, hydrological stress indices maps are compared with ODB geo-referred maps. In addition, an objective analysis is carried out by applying both statistical dichotomous and continuous scores.

3.1 Statistical dichotomous analysis

Primarily, the indices grid map was spatially co-located with the hydrometers position by choosing the nearest grid-point to the station geographical coordinates after verifying the correspondence between the grid-point upstream drained area calculated by the CHyM model, with the real value declared in the official station registry (where available).

As for the time co-location, both water level and indices time series are hourly, and it might appear straightforward to investigate the potential thresholds exceedances by comparing the same time step. However, during a flood wave, it is not infrequent to have water level data corrupted by measurement errors during the flood wave transition (i.e.: a solid surface stationing for a certain period under the hydrometric sensor). For this reason, the time location is carried out by associating a mobile interval of three hours (the target time step ± 1) of observations to each index time step. The choice of this confidence interval is arbitrary, although it is based on the authors' experience. The contingency table was then built, for each station point and for each index, considering the match between the co-located moderate hydrometric threshold exceedances (THR 2 in table 1) and the moderate indices threshold exceedances. Differently from water level thresholds, CAI and BDD indices thresholds have the same value for all the grid-points of the drainage network. These numerical thresholds are 6 mm/hour for BDD and 60 mm/day for CAI, respectively: the choice of these values is justified *a-posteriori* considering the performances of the proposed indices for different analysed severe events, during 10 years of operational activity (Colaiuda et al., 2020).

Under the most natural conditions and with continuous updating of the hydrometric thresholds depending on the morphodynamic variability of the basin, the proposed threshold levels for BDD and CAI should appear very close to the water level threshold for the specific site.

The dichotomous scores include the accuracy (A), the probability of detection (POD), the false alarm ratio (FAR). To build such a table, a flood event is considered as an observed "yes/no" event if the water level exceeds/does-not-exceed the empirical threshold; a flood event is an estimated "yes/no" event if the estimated index exceeds/does-not-exceed the BDD and CAI thresholds (Table 3). *A*, *POD* and *FAR* scored are defined as follows:

$$A = \frac{H+CN}{H+M+FA+CN} \tag{3.1.1}$$

$$POD = \frac{H}{H+M} \tag{3.1.2}$$

$$FAR = \frac{FA}{H+FA} \tag{3.1.3}$$

The calibration of the indices thresholds was chosen to maximize the hit rate *H*, though at the cost of a higher average false alarm rate: choosing a lower threshold increase detection skills of events with high uncertainty, according to Alfieri et al. (2019). All listed scores range from 0 to 1, where 1 is the optimal value for *A* and *POD*, while 0 indicates the best possible score for FAR.

3.2 Catch Rate

The Catch Rate (CR) was estimated for each index, to investigate effectiveness in detecting or missing correct flood warnings. To this aim, the orange (moderate) hydrometric level threshold exceedances (THR2) were chosen as a term of comparison with the corresponding moderate CAI and BDD indices thresholds. A match occurs when the hydrometric THR2 is exceeded and the moderate index threshold is exceeded, or, when the hydrometric THR2 is not exceeded and the moderate index threshold is not exceeded, within a 24 hours time range. A Boolean value 0/1 is then assigned when a match occurs. CR is calculated as the ratio between the number of correct matches found and the total number of analysed stations *N*:

$$CR = \sum_{i=1}^{N} \frac{1}{N} CESA_i \tag{3.2.1}$$

Where the acronym *"CESA"* stands for Correct Estimated State of Alert for the *i*-sensor, which assumes value "1" when estimation matches observation, and "0" when that match does not occur.

3.3 Time Peak Analysis

In order to further evaluate the timing accuracy of the BDD and CAI indices, all the available observed water level time series were compared to the indices time series. Because of the comparison between two different physical quantities, the chosen statistical scores are typically used for signal studies. The first statistical analysis was made through the calculation of the Lag Time Peak (LTP), to investigate the simultaneity of occurrence between the water level peak and the indices peak. According to the Italian Prime Minister Directive concerning "Operational guidelines for emergency management", issued on 3 December 2008, a lag time of "a few hours" (less than 12 hours) is estimated to be between an event occurrence and the activation of the Civil Protection Coordination Unit. In light of the above, we established that an adequate lag time peak for flood prediction should not exceed 3 hours. According to other authors (see, as an example Rabuffetti et al., 2008), the Relative Lag Time Peak (RLTP), defined as the ratio between LTP and the average time of concentration of the upstream basin, can be calculated.

3.4 Correlation Time Delay (CTD)

The cross correlation (CC) is typically used in the signal theory (Rabiner and Gold, 1975; Rabiner and Schafer, 1978; Benesty et al., 2004), for the assessment of similarity between two signals. Given two discrete series *x(t)* and *y(t)*, each one of *N* components, the cross correlation is calculated as the dot product of the series:

$$CC = \sum_{i=1}^{N} x(t_i) y(t_i) \tag{3.4.1}$$

The same product can be calculated, shifting the two signals of a time lag *L*:

$$CC(L) = \sum_{i=1}^{N} x(t_i) y(t_i + L) \tag{3.4.2}$$

The Correlation Time Delay (CTD) is then defined as the value of time lag *L* that maximizes the previous product.

$$CTD = \max_{L \in R} CC(L) \tag{3.4.3}$$

CTD represents an estimation of time shift between two series; therefore, we found this score to be suitable to measure the effectiveness of the signal given by the hydrological stress indices.

3.5 Derivate Dynamic Time Warping analysis

The Dynamic Time Warping (DTW, Berndt and Clifford, 1994; Keogh and Ratanamahatana, 2005; Maier-Gerber et al., 2019 and Di Muzio et al., 2019) allows to stress (or compress) two-time series to achieve a reasonable fit between them. The idea of the method is that the similarity between two sequences can be estimated by "warping" the time axis of one (or both) sequences, to achieve a better alignment. Although DTW has been successfully used in many domains, it may lead to obtaining wrong results; as an example, the technique may fail in finding the optimal alignment because a feature (i.e. peak or local minimum) in one sequence is higher or lower than its corresponding feature in the other sequence.

To overcome this problem, Keogh and Pazzani (2001) proposed the computation of warping using the local derivative of the time series to be compared and called this algorithm "Derivative Dynamic Time Warping" (DDTW).

The numerical procedure for the DTW calculation can be summarized as follows: given two discrete series *x(i)* and *y(j)* of *N* and *M* components respectively, an N-by-M matrix is built. An element *V(i,j)* contains the Euclidean distance between the i-*th* element of the first sequence and j-*th* element of the second sequence. For this matrix, a "warping" path *W* is defined as a contiguous set of *L* matrix elements, and the measure of misalignment *d* for the path *W* is given by:

$$d(W) = \frac{\sum_{i,j} V(i,j)}{\frac{1}{2}L(L-1)} \tag{3.5.1}$$

where the sum in the numerator is carried out over all the elements belonging to the warping path *W*. The denominator is used to normalize different length sequences. The DTW index is then calculated as the minimum value of *d(W)*, considering all the possible path *W*.

$$DTW = \min_{W} \; d(W) \tag{3.5.2}$$

For instance, if the two considered sequences are aligned and have the same number of components (*N=M*), the optimal path will be the *N* diagonal elements of matrix *V*.

The DDTW (Figure 5) algorithm implementation replaces the data time series with their first derivative and the Euclidean distance is measured on them. The first derivative has been calculated for each time series as follows

$$D(x[i]) = \frac{(x[i]-x[i-1])+((x[i+1]-x[i-1])/2}{2} \tag{3.5.3}$$

4 Study Area Description

The study area covers the Central Apennines District (Figure 1), with an extension of 42 506 km^2 and about 8 million inhabitants. The northern part, which includes the upstream basin of the Tiber river from the confluence with the Nera river, is characterized by a less dense draining network with respect to the lower part of the basin. This area has an extensive hydrography, characterized by both perennial rivers, constantly fed by groundwater, and seasonal streams, which are activated only in rainy periods. Moreover, plenty of artificial reservoirs and hilly ponds uptake surface runoff water. The Adriatic slope is located over the central part of the district, extending from upper Marche Region (Potenza River) to the southern part of Abruzzo Region (Sangro River). The lower path of the Tiber river is also part of this area, together with the tributaries on the left bank, from Nera to Aniene rivers.

This area is affected by inundations along major rivers, as well as flash floods in torrents and minor streams, especially on the heels of the ridge, where high-intensity rainstorms cause lowland flooding. Most portion of the drainage network is characterized by a significant water storage (with a quite constant spring flow rate during the year) and marked by hydroelectric power plants, built since the last century (Tiber Basin Authority, 2010). The peak discharge variation depends on the storage type: generally, the effect of a reservoir to flood control results from a combination of regulated and unregulated storage (Volpi et al., 2018). The former, used in the analyzed area, is less efficient in flood-peak reduction than regulated storage, as it begins filling even before it is needed. Moreover, the effect of a flood control reservoir depends on the combination of off-stream or on-stream detention ponds as reported by Ravazzani et al. (2014). Dams and reservoirs play an important role during flood events (Rodda, 2011; Kundzewicz et al., 2014; Ayalew et al., 2017; Habets et al., 2018): this role is not always favourable; they adversely affect the extent of an inundation due to dike breaches, blockage of bridges and culverts by debris. Anyway, weak coordination between different actors involved in water resources management may significantly affect flood dynamics. In multi-purpose reservoirs, competing interests represent a key issue in flood regulation: irrigation, hydropower generation and flood control generally compete, even when the reservoir is owned by a single country or agency. This conflict of interests is heightened, when the basin is interregional, as in the case of Central Apennines District. For those reasons, the WMO (2009) recommends to carefully evaluate the flood timing and dynamics.

5 Results and discussion

In this section, the analysis of a meteo-hydrological event occurred in Central Italy on 11^{th}-13^{th} November 2013 is proposed. The 3-days event was characterized by intense precipitation, involving the whole Central Apennines ridge and three different regions, progressively affecting the Adriatic side of the central part of Italy, moving from North to South. To better organize our analysis, the event was divided into three different case studies, related to three different regions involved: Umbria (CS01), Marche (CS02), and Abruzzo (CS03). The CHyM model simulations were set to three different geographical domains, as shown in Figure 6. The event was very intense and caused many damages and few fatalities in all regions: an overview of the phenomenon is reported in Table 2, where relevant information about observed effects and sources of information are provided.

Details of links pointing to each source used to organize ODB are provided in the supplementary materials, where all hit municipalities and affected rivers are also listed.

5.1 Synoptic Analysis

On November 11th, 2013, a large synoptic-scale meteorological system originated from the Atlantic Ocean and moved into the Mediterranean area. In particular, the cold air coming in from the Rhone door has induced rapid cyclogenesis on the Genoa Gulf. The barometric minimum moved southward along the Italian Peninsula and reached the Tyrrenian Sea on November 12th. The persistence of the occluded front over Italy caused heavy and long precipitation, initially affecting northern regions and, progressively, central and southern areas, as the minimum moved toward the Lybian coasts, on November 13th. The precipitation was widespread, with a huge amount. According to the event reports from Regional Civil Protection authorities, registered precipitation amounts were almost than 300 mm/72 hours in several areas, mainly located along the Apennines ridge, between Marche and Umbria regions (Figure 7).

5.2 Case Studies Analysis

Hydrological simulations were carried out over a geographical domain larger than the areas where floods were actually observed, in order to verify the absence of predicted hydrological stress conditions in those areas where hydrological criticalities did not occur. Hydrological simulation was set by using a spin-up time of 120 hours for all case studies, before the day of the hydrological event. Given the small extension of the involved catchments, 120 hours of spin-up seems to be enough for the model initialization. It should be noticed that stress indices are used to detect hydrological situations where relevant discharges, driven by significant rainfall events in short time (few hours to few days) are present. The selected case studies affected different regions of Central Italy characterized by catchments of different sizes and geomorphological characteristics, allowing the evaluation of indices feasibility in heterogeneous domains. Spatial and temporal characteristics of the hydrological simulations are reported in Table 4.

As discussed in section 3, the ODB information about case studies were geo-referenced on a Google Earth maps (Figure 2, 3, 4). The cyan waves symbols indicate reported inundations, and the pinpoints show the hydrometers displacement: the colour assigned to each pinpoint highlights the observed state of alert, namely, the hydrometric threshold exceedances (see Table 1 for further details). In the same map, the drainage network is represented by blue lines; white lines indicate alert zone boundaries, defined by Civil Protection, reddish areas encompass the administrative boundaries of the main affected municipalities (i.e., where a flood was reported), while the small cyan triangles highlight the main water reservoirs located inside the domain. In Figure 2 and 3, red rectangles represent the flood affected area published on Copernicus Emergency Management Service Platform (EMS Rapid Mapping Activations (EMSR060): https://emergency.copernicus.eu/mapping/list-of-components/EMSR060).

5.2.1 Case study 1: Umbria Region

From November 11th to 12th, 2013, a severe weather event hit the Umbria Region. The event mainly concentrated over the North-eastern part of the region, along the administrative boundary with Marche Region. According to the data provided by the official hydro-meteorological monitoring network, precipitation was persistent and intense, resulting in exceptional amounts, up to 440 mm in the Castelluccio di Norcia station and 330 mm in Gualdo Tadino, in 72 hours (see Figure 7). Floodings affected main rivers, as well as small catchments (river outlet highlighted in Figure 2), such as the Tiber, the upper Chiascio, and the Topino basins. In particular, the flooding on the Sentino river, flowing along the boundary with the Marche region, caused damages on 12 residential buildings and temporarily isolated the Branca Hospital, due to considerable roads and bridges disruption. All municipalities of the Apennines ridge registered damages. A flood wave occurred over the Nera river and the Corno tributary. According to the Civil Protection official report, Montedoglio and Corbara dams played a crucial role in the flood wave lamination and phase shifting in the Tiber River and Casanuova dam in the Chiascio river, respectively (Figure 2, cyan triangles). The initial value of water in the two reservoirs is not considered, because no data are provided about release and withdrawals of water from the water reservoirs. Due to the lack of water storage data, it is not possible to properly assess the flow discharge simulation, therefore, we can only state that the discharge simulation from our model differs from observations and highlight the presence of an anthropic impact due to artificial water reservoirs displaced upstream. According to our experience, we have found that indices peak timing and their shifts respect to observed hydrometric level can provide information about the flood management through water reservoirs release and withdrawals, that are able to postpone (or anticipate) discharge maxima propagation downstream.

For this first Case study (CS01, Figure 6), the main characteristics of hydrological simulation are reported in Table 4. The hydrological model has been forced with observed precipitation data from almost 370 rain gauges, located in the geographical domain. The CAI and BDD indices maps obtained for CS01 are shown in Figure 8. Hydrological stress indices are computed at hourly time steps. However, the map refers to a 24 hours time interval, where the maximum daily value of the index is assigned to each grid-point. In other words, the map gives an idea of the maximum stress conditions that may occur in the whole day. Moreover, the actual drainage network is denser in the highlighted catchments, however, we decided to plot only grid-points having a drained area larger than 15 km^2, to improve the map visualization and interpretation.

A qualitative comparison of Figures 2 and 8 allows to identify similarities in the hydrological stress spatial distribution and observed inundations. The higher CAI and BDD stresses degree is mainly given in the north-eastern side of drainage network, from the upper Umbria regional boundary and along the slope exposed to the Adriatic side. All the reported damages and orange/red hydrometric levels are observed in the same area. The western side of Umbria was not significantly affected by the event and no relevant stress degree is given by indices.

The CAI index overestimates the hydrological stress extension in the south-eastern part of the region, near the boundary with the Lazio region. Moreover, a difference between the two indices needs to be highlighted: the BDD index stress degree is lower in the minor drainage network, and relevant in the main river channel. This effect is due to the different nature of the

indices and the different physical quantities considered in their calculation: the CAI index is directly linked to the precipitation rate, resulting in higher responsiveness in the smallest river channels, where the high peak precipitation-driven flood is the predominant mechanism for inundations. On the other hand, the BDD index calculation is based on the discharge value and responsive to runoff-driven floods, resulting from the combination of different hydrological processes, such as rainfall-runoff, infiltration, soil moisture and melting.

Besides the spatial assessment, timing analysis is given through a heterogeneous comparison between hydrometric level time series and indices time series (Figure 9), for six relevant hydrometric stations located in the upper part of Umbria region, where the orange hydrometric threshold was exceeded. The represented quantities, as well as the associated thresholds, are normalized. Indices increasing and decreasing rates show a similar behaviour with the hydrometric level trend, and maxima occurrence is concomitant in Tiber and Topino river stations and slightly anticipated (from 3 to 6 hours) by the indices in Chiascio, and Nera rivers.

As stated at the beginning of this paragraph, artificial water storage and lamination played an important role in the flood wave management in this area. Flood abatement is achieved by detaining and later releasing a portion of the peak flood flow (WMO, 2009) and different kinds of reservoirs have been found to cause different release dynamics.

Focusing our analysis on the Pianello station (Figure 9d), downstream of the Casanuova dam, the indices peak shifting may be due to lamination of flood wave by the on-stream water storage system. The presence of the Montedoglio dam, upstream Tevere-Santa Lucia and Tevere-Petrantonio stations (Figure 9 a and b) does not produce the same effect and peaks timing appears concomitant with the hydrometric level peak. Although the dam has retained almost all of the inflows from the upstream basin (up to 13th November at 12UTC), its off-stream position allowed the regulation of the intensity of the flood, rather than its timing (Figure 9a, b)). The increasing hydrometric profile after 13th November 2013, 12 UTC, indicates the artificial release after the end of the event.

Despite the presence of large and small detection storages affecting the indices accuracy, the average CR value, calculated over 22 hydrometric stations is 0.86 for BDD and 0.77 for CAI. This result supports the qualitative analysis discussion, where a spatial correspondence between the indices map and the ODB map was observed.

Threshold exceedances hourly match have been calculated over the same 22 hydrometric stations, belonging to 7 different catchments, for a total amount of 2574 hours analysed (120 hours per station); resulting scores are summarized in table 5 (scores breakdown for each station are not shown). The accuracy of the prediction is above 0.8 for both indices, while the POD is around 0.7 for BDD and 0.5 for CAI. False Alarm Rate is around 0.45 in both cases, however, when the flood dynamics are artificially regulated, the misalignment between observed and simulated peaks, analysed in Figure 9 discussion, leads to increasing values of FAR. The indices stress overestimation may be attributable to missing territorial information, however, without evidences in that way, we can only assess that the model did not properly simulate hydrological stress.

As for the timing analysis, resulting LTP is <1 hour for BDD and about -7 hours for CAI index. In general, all timing scores resulted to be better for BDD than CAI index, with a slight tendency to anticipate the peak values.

5.2.2 Case study 2: Marche Region

The official report of the Marche Region Civil Protection described the occurrence of many hydrological criticalities over the whole region, especially in the inner areas, along the Apennines ridge, where maxima rainfall were registered. Precipitation peaks were up to 487 mm in 72 hours in Pintura di Bolognola rain gauge (South-East of the region) and 200 mm in Conca_1 (North-East of the region) (Figure 7). Floods affected many rivers in the upper Marche: critical situation over the Metauro basin was recorded over the upstream tributaries (Candigliano, Bosso, and Burano rivers). Other floods were also recorded in the Cesano, Misa, and Arzilla basins, as well as the Chienti river, where a flood wave propagated, starting from the upper tributaries Fiastrone and Fiastra. On the Foglia basin, the Mercatale dam laminated part of the flood since early hours of November 11th, until the afternoon, when its accumulation capacity finished. The upper part of the Potenza, Tenna and Tronto basins were also affected by floods.

A qualitative analysis of the hydrological stress spatial distribution by comparing ODB data (Figure 3) and indices maps (Figure 10) was carried out, to identify a geographical match between recorded inundations and simulated hydrological stress. For this case study (CS02, Figure 6), the main characteristics of hydrological simulation are summarized in Table 4.

The hydrological model has been forced with almost 138 rain gauges data, used to rebuild the precipitation field. Main affected municipalities lay on the piedmont areas of the Apennines' ridge (the lower part of Figure 3), where maxima precipitation was registered. However, the flood wave originating from those areas propagated downhill, toward the Adriatic Sea, affecting all the river systems, where damages, inundations occurred, and hydrological level criticality threshold were exceeded. The CAI index map (Figure 10b) has identified almost each grid-point of the drainage network with the highest stress degree, while in the BDD map maximum stress over the main rivers (Figure 10a) is highlighted. The difference between the two indices behaviour is due to the same mechanism described for CS01.

In Marche region, many dams affect the natural river flow. The normalized indices and hydrometric levels profiles are shown in Figure 11: the effect of Mercatale dam lamination caused a progressively larger hydrometric peak shifting along the Foglia river (Figures 11c and 11d). The precipitation resulted in high supplies to the reservoirs of the Metauro, Chienti and Tronto basins where it was necessary to retain part of the inlet flow during the event. Where the storage capacity allowed to manage the amount of precipitated rain, a rolling service was carried out. Maximum peak shifting is shown in Figure 11f, for the Fiastrone station. A first hydrometric peak is slightly postponed by indices, while a same-magnitude secondary peak is weakly detected. A relevant impact on Fiastrone station is determined by the presence of unregulated on-stream storage from the Fiastra lake, which is the largest hydroelectric basin in the Marche region. The other time series shown in Figure 11 are characterized by a synchronous peak of indices and hydrometric level. Dichotomous and continuous analysis scores for CS02 are shown in Table 5: for this case study, 28 stations time series have been analyzed, covering 13 different basins. In this case, an Accuracy of 0.8 is reported for both indices, being the POD around 0.70 for BDD and 0.55 for CAI. A FAR score of 0.37 for BDD and 0.43 for CAI has been calculated. LTP is less than one hour for BDD and -4 hours for CAI index, resulting in a RLTP of 0.05 for BDD and -0.56 for CAI index. CTD is significantly lower in BDD respect to CAI index, with values of -1.4

and -5.6, respectively. The DDTW results to be 0.04 for BDD and 0.06 for CAI index. Indices response on dichotomous scores (CR) is found to be similar, however, timing scores are quite different, resulting in slight anticipation of peak values in the CAI index. Worst scores are obtained on the Fiastrone river, heavily impacted by the Fiastra dam lamination. The effect on indices timing is relevant since the flood wave is simulated to occur 22 hours in advance for the BDD and 32 for the CAI. For this station, despite values for FAR ranging from 0.56 for CAI to 0.56 for BDD, the POD scores are 0.94 and 0.66, respectively.

5.2.3 Case study 3: Abruzzo Region

In the Northern and Central part of Abruzzo region, a precipitation amounts up to 400 mm in 72 hours were recorded in Pretara rain gauge and 280 mm in Castel del Monte, over the inner, mountainous area (Figure 7).

Main affected rivers (from North to South) were Salinello, Tordino, Vomano, Piomba, Saline (included its tributaries Fino and Tavo), and Pescara, the latter one being the widest catchment of the region with a drained area of 3190 km^2. All aforementioned catchments, as well as the whole Abruzzo region territory, is disseminated by plenty of water withdrawals: according to ISPRA (2018), 14 relevant dams retain a total amount 370.38 mln m^3 of water from the drainage network. An undefined number of minor withdrawals is still under census by the local authorities (Abruzzo Region Deliberation no. 435/2016) and the total magnitude of the water uptake is still difficult to assess.

Flood events for this case study affected the road networks, industrial settlements, scattered houses located along the river paths and in depressed areas. Flood waves also occurred in the southern part of the region although they did not have significant effects. Main setting of CS03 (Figure 6) are summarized in Table 4. The hydrological model assimilated data from 135 rain gauges from the official network. The comparison between indices 24 hours maps (Figure 12) and ODB observation spatial distribution (Figure 4) reveals a correspondence between the most damaged area, involving all the North of Pescara river system and the highest hydrological stress, highlighted by the indices reddish colours. However, the CAI index map also shows high hydrological stress in those southern watersheds, where inundations are not reported. On the other hand, according to the BDD map, no relevant stress is detected in this area. Moreover, the smallest tributaries were not highlighted by the latter index, coherently with CS01 and CS02 findings. In Figure 13, six relevant normalized time series of hydrometric levels and indices are reported. Tordino, Pescara, and Vomano stations show peak shifting, due to the presence of many dams along the rivers path. For example, the Aterno-Pescara catchment hosts at least 7 different dams, concentrated in a drained area of barely 3100 km^2. The induced flood shift may be even in the order of more than one day (e.g. 30 hours delay in Pescara a Villareia station, Figure 11f). Picciano and Fino are small watersheds, not impacted by human activity in terms of water uptake: in this case timing scores assumes lower values (LTP and CTD about 2 hours for BDD and -1 hour for CAI, with RLTP of -0.29 and -0.14, respectively). DDTW results to be 0.09 for BDD and 0.11 for CAI.

Among all the sensors analyzed, the indices reported the right state of criticality for about 77% of them (CR scores, Table 5). The timing analysis is given for 26 hydrometric time series, located over 16 different river basins. The overall Accuracy for CS03 is more than 0.9 for both indices, with a higher POD for BDD (0.81), than for CAI (0.72). However, the latter shows a

slightly lower FAR. LTP is about -8 hours for BDD and -12 for CAI, resulting in RLTP of -1.1 for BDD and -1.6 for CAI. The Correlation Time Delay is lower for BDD than for CAI (-4.2 and -7.5, respectively), while the DDTW is very low for both the proposed alarm indices, as it is 0.09 for BDD e 0.1 for CAI. Obtained results suggest that almost all floodings were predicted by both indices, even if the timing analysis reveals slight anticipation, probably due to the artificial water management effect.

6 Conclusions

This work focused on flood prediction through the application of end users-oriented indices, able to identify segments of drainage network susceptible to flood. Several hydro-meteorological severe events, collected during the CETEMPS operational activity, were used to calibrate two hydrological indices thresholds, starting from the calculation schemes of the CHyM model. The use of deterministic models for hydrological forecast involves a series of critical points. First of all, the need to calibrate and validate the model outputs with a very long time series of hydrological quantities, mainly represented by discharge data. However, these data are not always available, in particular, on small seasonal streams that are not remotely monitored, but frequently hit by destructive flooding phenomena. Since floodings are complex events, depending on several processes, it is not straightforward to establish a flow discharge threshold value, beyond which the river can be considered susceptible of flood. For this reason, many developed hydrological thresholds are site-specific and not generally applicable over different areas, other than the river sections where they have been calibrated. The two proposed CAI and BDD indices were validated on a case study basis, through the analysis of an extreme weather event affecting Central Italy on 11^{th}– 13^{th} November 2013. The 3-days event was simulated by the Cetemps Hydrological Model, forced with observed raingauges data, over three different geographical domains encompassing Umbria and Tiber basin, Marche, and Abruzzo regions. Indices formulations followed two different approaches: the BDD index is based on the ratio between the computed (natural) discharge and the square of hydraulic radius, while the CAI index is more empirical, representing the amount of the precipitation drained by each grid-point of the drainage network, in a time interval corresponding to the mean time of concentration of the upstream area. Three thresholds have been set for each index and calibrated in order to obtain a qualitative correspondence between the indices and the hydrometric thresholds exceedances, defined by each Regional Civil Protection Functional Centre. A colour-code, similar to those used for the hydrogeological criticality assessment, was then assigned to each threshold, with the aim of simplifying index signal interpretation by Civil Protection end-users. The forecast skill of both indices has been investigated at station level, through dichotomous and continuous statistical analysis, by comparing indices time evolution and hydrometric level time series, taking advantage of typical assessment methods used in the signal theory, such as the derivative dynamic time warping. Moreover, spatial information given by both indices was assessed by comparing daily BDD and CAI stress maps and localization of effects at ground, collected from event reports, press releases and warnings. Obtained results indicated as the hydrological stress spatial information, highlighted by higher indices values, is coherent with the localization of affected municipalities and flood reports, while no stress overestimation is reproduced over those areas not involved in the event. Objective dichotomous statistical analysis was performed over 78 hydrometric stations by using contingency tables, built by

comparing indices and hydrometric height moderate threshold exceedances. Results evidenced high accuracy, with values exceeding 0.8 for both indices and all CSs. False alarm rates were under 0.5, while appreciable difference is given by the probability of detection ranging from 0.51 for CAI to 0.80 for BDD among the different case studies. Signal analysis has been carried out over 120 hours time series of indices and observed river stages. The DDTW over all stations was found to be abundantly lower than 0.1, which is commonly referred as the threshold value beyond which two signals can be considered independent. Even if the stress signal behaviour is correctly reproduced by both indices, peak timing analysis showed some anticipation in signal peak occurrences in the order of few hours. Timing bias is more pronounced for the CAI index, where displacements of more than - 4 and up to about - 7 hours are highlighted by all statistical parameters. As mentioned, validation scores were calculated considering all available hydrometers in the domain, however, it should be highlighted as many stations as possible among them, are placed downstream to dams. Therefore, in these points, flood propagation is heavily influenced by retention and release from artificial water storage, which is widespread over the considered geographical domain, heavily exploited in terms of hydroelectric power production. Indices performance would benefit of potential availability of retention and release data, however, the main aim of developing general thresholds for the proposed indices deals with contemplating data scarcity and hypothesis of unavailability of information about water uptake, which is very difficult to find, in the author's experience. As for indices applicability, results highlighted a different indices response to different catchments and diverse flooding dynamics. According to Chen et al. (2010), floods may have different drivers: fluvial floods are mainly determined by the limited capacity of drainage systems, while pluvial floods are caused by deluges from river channels. However, the discrimination between a pluvial and a fluvial flood is not sharp; in the matter of fact, most events result in a combination of both processes. This condition often affects small hydrological basins, such as most Italian rivers (drained area lower than 10000 km^2, according to the definition provided by Chapman, 1992). According to the underlined differences found in CAI and BDD mapping, the proposed indices gives complementary information about hydrological stress over wide areas, as the former index appears to be more responsive to predominant pluvial flood dynamics affecting smallest tributaries, while higher stress identified by BDD occurs over main channels.

Acknowledgements

The present paper is written in the framework of the Agreement between the Centre of Excellence CETEMPS and the Functional Centre of Abruzzo Region. The authors would like to thank colleagues from the Civil Protection Dept. of Abruzzo for their feedback during the activities foreseen in the agreement and Francesca Sini (from Civil Protection Dept. of Marche) for comments that improved the manuscript. Moreover, part of this work is financed by the PON-AIM project, funded by the Italian Ministry of University and Research (MUR).

Authors' contribution

Conception and design: A. L., V. C., B. T.; Analysis: A. L., B. T., V. C.; Manuscript writing: A. L., V. C., B. T., M. V.; Draft revision: V. C., B. T., A. L.; Coordination: B. T.

References

Abruzzo Region Council Deliberation no. 659/2017, Att. A: “Sistema di Allertamento Regionale Multirischio” (document in Italian), http://bura.regione.abruzzo.it/singolodoc.aspx?link=2018/Speciale_114_0.html; last access: 11 June 20202, 2018.

Ahn, J. H. and Il Choi, H.: A New Flood Index for Use in Evaluation of Local Flood Severity: A Case Study of Small Ungauged Catchments in Korea, J. Am. Water Resour. Assoc., 49, 1–14, https://doi.org/10.1111/jawr.12025, 2013.

Alfieri, L., Velasco, D., and Thielen, J.: Flash flood detection through a multi-stage probabilistic warning system for heavy precipitation events, Adv. Geosci., 29, 69–75, https://doi.org/10.5194/adgeo-29-69-2011, 2011.

Alfieri, L., Salamon, P., Pappenberger, F., Wetterhall, F., and Thie-len, J.: Operational early warning systems for water-related hazards in Europe, Environ. Sci. Policy, 21, 35–49, https://doi.org/10.1016/j.envsci, 2012.

Alfieri, L., Pappenberger, F., and Wetterhall, F.: The extreme runoff index for flood early warning in Europe, Nat. Hazards Earth Syst. Sci., 14, 1505-1515, https://doi.org/10.5194/nhess-14-1505-2014, 2014.

Alfieri, L., Burek, P., Feyen, L., and Forzieri, G.: Global warming increases the frequency of river floods in Europe, Hydrol. Earth Syst. Sci., 19, 2247–2260, 2015.

Alfieri, L., Berenguer, M., Knechtl, V., Liechti, K., Sempere,-Torres, D., and Zappa, M.: Flash Flood Forecasting Based on Rainfall Thresholds. In: Duan Q., Pappenberger F., Wood A., Cloke H., Schaake J. (eds) Handbook of Hydrometeorological Ensemble Forecasting. Springer, Berlin, Heidelberg, 2017.

Apel, H., Martínez Trepat, O., Hung, N. N., Chinh, D. T., Merz, B., and Dung, N. V.: Combined fluvial and pluvial urban flood hazard analysis: concept development and application to Can Thocity, Mekong Delta, Vietnam, Nat. Hazards Earth Syst. Sci., 16, 941–961, https://doi.org/10.5194/nhess-16-941-2016, 2016.

Ashley, R. M., Balmforth, D. J., Saul, A. J., and Blanskby, J. D.: Flooding in the future - predicting climate change, risks and responses in urban areas, Water Science and Technology, 52(5), 265-273, 2005.

Ayalew, T. B., Krajewski, W. F., Mantilla, R., Wright, D. B., and Small, S. J.: Effect of spatially distributed small dams on flood frequency: insights from the soap creek watershed, J. Hydrol. Eng., 22 (7), 04017011, 2017.

Balmforth, D., Digman, C. J., Butler, D., and Shaffer, P.: Defra Integrated Urban Drainage Scoping Study Report, Department for Environment, Food and Rural Affairs, Flood Management Division, 2006.

Basha, E. and Rus, D.; Design of early warning flood detection systems for developing countries, Inform. Commun. Technol. Dev., IEEE, 1–10. 2007.

Bates, B. C., et al.: Climate change and water. Technical paper of the Intergovernmental Panel on Climate Change, Geneva: IPCC Secretariat, 2008.

Benesty, J., Chen, J., and Huang, Y.: Time-delay estimation via linear interpolation and cross correlation, IEEE Transactions on Speech and Audio Processing, vol. 12, no. 5, 2004.

Berenguer, M., Corral, C., Sanchez-Diesma, R., and Sempere-Torres, D.: Hydrological validation of a radar-based nowcasting technique, J. Hydrometeorol., 6, 532-549, 2005

Berndt, J. B. and Clifford, J.: Using Dynamic Time Warping to Find Patterns in Time Series, AAAIWS'94 Proceedings of the 3rd International Conference on Knowledge Discovery, 359-370, 1994.

Berz, G., Kron, W., Loster, T., Rauch, E., Schimetschek, J., Schmieder, J., Siebert, A., Smolka, A., and Wirtz, A.: World Map of Natural Hazards – A Global View of the Distribution and Intensity of Significant Exposures, Natural Hazards, 23, 443–465, 2001.

Blöschl et al.: Changing climate shifts timing of European floods, Science, 357 (6351), 588–590, doi: 10.1126/science.aan2506, 2017.

Blöschl, G., Hall, J., Viglione, A. et al.: Changing climate both increases and decreases European river floods, Nature, 573, 108–111, https://doi.org/10.1038/s41586-019-1495-6, 2019.

Braca, G., Bussettini, M., Lastoria, B., and Mariani, S.: Linee guida per l'analisi e l'elaborazione statistica di base delle serie storiche di dati idrologici, no. 84/13, ISPRA, ISBN: 978-88-448-0584-5, 2013.

Borga, M.: Accuracy of radar rainfall estimates for streamflow simulation, Journal of Hydrology, 267, 26–39, 2002.

Brandolini, P., Cevasco, A., Firpo, M., Robbiano, A., and Sacchini A.: Geo-hydrological risk management for civil protection purposes in the urban area of Genoa (Liguria, NW Italy), Nat. Hazards Earth Syst. Sci., 12, 943–959, doi:10.5194/nhess-12-943-2012, 2012.

Chapman, D.: Water quality assessment. In: Chapman, D. (Ed.), on behalf of UNESCO, WHO and UNEP, Chapman & Hall, London, 585pp, 1992.

Chen, A. S., Djordjevic, S., Leandro, J., and Savic, D. A.: An analysis of the combined consequences of pluvial and fluvial flooding, Water Science and Technology, 62(7), 1491-1498, doi:10.2166/wst.2010.486, 2010.

Cloke, H. L. and Pappenberger, F.: Evaluating forecasts of extreme events for hydrological applications: an approach for screening unfamiliar performance measures, Meteorological Applications, 15, 181-197, doi: 10.1002/met.58, 2008.

Colaiuda, V., Lombardi, A., Verdecchia, M., Mazzarella, V., Ricchi, A., Ferretti, R. and Tomassetti, B.: Flood Prediction: Operational Hydrological Forecast with the Cetemps Hydrological Model (CHyM), Int J Environ Sci Nat Res., 24(3): 556137, doi: 10.19080/IJESNR.2020.23.556137, 2020.

Coppola E, Verdecchia M, Giorgi F, Colaiuda V, Tomassetti B, Lombardi A.: Changing hydrological conditions in the Po basin under global warming. Sci Total Environ., 2014.

Coppola, E., Tomassetti, B., Mariotti, L., Verdecchia, M., and Visconti, G.: Cellular automata algorithms for drainage network extraction and rainfall data assimilation, Hydrolog. Sci. J., 52, 579– 592, 2007.

Corral, C., Berenguer, M, Sempere-Torres, D., Silvestro, F., Poletti, L., and Rebora, N.: Comparison of two systems for regional flash flood hazard assessment, J. Hydrol., 572, 603-619, 10.1016/j.jhydrol.2019.03.026, 2019.

Dankers, R. and Feyen, L.: Flood hazard in Europe in an ensemble of regional climate scenarios, J. Geophys. Res., 114, D16108, doi:10.1029/2008JD011523, 2009.

Di Baldassarre, G. and Montanari, A.: Uncertainty in river discharge observations: a quantitative analysis, Hydrol. Earth Syst. Sci., 13, 913–921, https://doi.org/10.5194/hess-13-913-2009, 2009.

Di Baldassarre, G. and Claps, P.: A hydraulic study on the applicability of flood rating curves, Hydrology Research, 42 (1), 10–19, https://doi.org/10.2166/nh.2010.098, 2011.

Di Muzio, E., Riemer, M., Fink, A. H., and Maier-Gerber, M.: Assessing the predictability of Medicanes in ECMWF ensemble forecasts using an object-based approach, Quarterly Journal of the Royal Meteorological Society,145:720, 1202-1217, 2019.

Eckstein, D., Künzel, V., Schäfer, L., and Winges, M.: Global Climate Risk Index 2020, Germanwatch, available online: www.germanwatch.org/en/cri , ISBN 978-3-943704-77-8, last access: 11 June 2020, 2019.

European Parliament. Directive 2007/60/Ec of the European Parliament and of the Council of 23 October 2007 on the assessment and management of flood risks. http://eur-lex.europa.eu/en/index.html, 2007.

Fassi, P., Molari, M., Cucchi, A., Valsecchi, I. and De Antoni, F.: Quaderni tecnici del Centro Funzionale - Soglie idrometriche, https://www.researchgate.net/publication/305303520_Quaderni_tecnici_del_Centro_Funzionale__Soglie_idrometriche, document in Italian), last access: 11 June 2020, 2008.

Feyen, L., Dankers, R., Bódis, K. et al.: Fluvial flood risk in Europe in present and future climates, Climatic Change, 112, 47-62, https://doi.org/10.1007/s10584-011-0339-7, 2012.

Field, C. B., et al.: Managing the risks of extreme events and disasters to advance climate change adaptation. Special Report of Working Groups I and II of the Intergovernmental Panel on Climate Change (IPCC), Cambridge: Cambridge University Press., 2012.

Giorgi, F.: Climate change hot-spots, Geophys. Res. Lett., 33, 8707, doi:10.1029/2006GL025734, 2006.

Giorgi F. and Lionello P.: Climate change projections for the Mediterranean region, Glob. Planet. Change, 63, 90–104, 2008.

Habets, F., Molénat, J., Carluer, N., Douez, O., and Leenhardt, D.: The cumulative impacts of small reservoirs on hydrology: A review, Science of The Total Environment, 643, 850–867, https://doi.org/10.1016/j.scitotenv.2018.06.188, 2018.

Hapuarachchi, H. A. P., Wang, Q. J., and Pagano, T. C.: A review of advances in flash flood forecasting, Hydrol. Process, 25, 2771–2784, 2011.

Head of Italian National Civil Protection Depatrment: Indicazioni operative recanti “Metodi e criteri per l’omogeneizzazione del Sistema di allertamento nazionale per il rischio meteo-idrologico e idraulico e della risposta al Sistema di protezione civile”, Communication Note (document in Italian), http://www.protezionecivile.gov.it/documents/20182/823803/Nota+del+Capo+Dipartimento+alle+Regioni+e+Province+Autonome/7c4ad941-1d1e-4a3c-861a-7652408f2302 (document in Italian), last access: 11 June 2020, 2016.

Horlick-Jones, T., Amendola, A., and Casale, R.: Prospect for a coherent approach to Civil Protection in Europe. Natural risk and Civil Protection, E &FN Spon, London, 1–12, 1995.

Hurford, A., Priest, S., Parker, D., and Lumbroso, D.: The effectiveness of Extreme Rainfall Alerts in predicting surface water flooding in England and Wales, Int. J. Climatol., 32, 1768–1774, https://doi.org/10.1002/joc.2391, 2012.

ISPRA, Invasi Artificali – Edizione 2018, Report; https://annuario.isprambiente.it/ada/basic/6869" \h, (document in Italian), last access: 12 June 2020, 2018.

Italian Civil Protection Department, CIMA Research Foundation: The Dewetra Platform: A Multi-perspective Architecture for Risk Management during Emergencies. In: Hanachi C., Bénaben F., Charoy F. (Eds.), Information Systems for Crisis Response and Management in Mediterranean Countries. ISCRAM-med 2014. Lecture Notes in Business Information Processing, Cham: Springer, pp. 165-177, 2014.

Jain, S. K., Mani, P., Jain, S. K., Prakash, P., Singh, V. P., Tullos, D., Kumar, S., Agarwal, S. P., and Dimri, A. P.: A Brief review of flood forecasting techniques and their applications, Int. J. River Basin Man., doi:10.1080/15715124.2017.1411920, 2018.

Javelle, P., Fouchier, C., Arnaud, P., and Lavabre, J.: Flash flood warning at ungauged locations using radar rainfall and antecedent soil moisture estimations, J. Hydrol., 394, 267–274, 2010.

Keogh, E. J. and Pazzani, M.: Derivative Dynamic Time Warping, Proceedings of First SIAM International Conference on Data Mining, ISBN: 978-0-89871-495-1, 2001.

Keogh, E. J. and Ratanamahatana, C. A.: Exact indexing of dynamic time warping, Knowledge and Information Systems, 7(3), 358-386, doi: 10.1007/s10115-004-0154-9, 2005.

Krzhizhanovskaya, V. V., Shirshov, G. S., Melnikova, N., Belleman, R., Rusadi, F. I., Broekhuijsen, J., Gouldby, B., Lhomme, J., Balis, B., Bubak, M., Pyayt, A., Mokhov, I., Ozhigin, A. Lang, B., and Meijer, R.: Flood early warning system: Design, implementation and computational modules. Procedia Computer Science, 4, 106-115, doi: 10.1016/j.procs.2011.04.012, 2012.

Kundzewicz, Z. W. and Schellnhuber H.-J.: Floods in the IPCC TAR Perspective, Natural Hazards, 31, 111–128, https://doi.org/10.1023/B:NHAZ.0000020257.09228.7b, 2004.

Kundzewicz, Z. W.: Changes in Flood Risk in Europe, IAHS Special Publication 10, IAHS Press, Wallingford, 516, 2012.

Kundzewicz, Z. W., Kanae, S., Seneviratne, S., Handmer, J., Nicholls, N., Peduzzi, P., Mechler, R. M., Bouwer, L. M., Arnell N., Mach, K., Muir-Wood, R., Brakenridge, G. R., Kron, W., Benito, G., Honda, Y., Takahashi, K., and Sherstyukov, B.: Flood risk and climate change: global and regional perspectives, Hydrological Sciences Journal, 59:1, 1-28, doi: 10.1080/02626667.2013.857411, 2014.

Lehmann, E.: Extreme rain may flood 54 million people by 2030, Sci. Am: https://www.scientificamerican.com/article/extreme-rain-may-flood-54-million-people-by-2030/, last access: 11 June 2020, 2015.

Lighthill, M.J. and Whitham, C. B.: Proceedings of the Royal Society, London, Ser. A 1995; 229, 281–316, ISBN 978-3-943704-77-8, 1992.

Llasat, M. C., Llasat-Botija, M., Prat, M. A., Porcú, F., Price, C., Mugnai, A., Lagouvardos, K., Kotroni, V., Katsanos, D., Michaelides, S., Yair, Y., Savvidou, K., and Nicolaides, K.: High-impact floods and flash floods in Mediterranean countries: the FLASH preliminary database, Adv. Geosci., 23, 47-55, 2010.

Maier-Gerber, M., Riemer, M., Fink, A. H., Knippertz, P., Di Muzio, E., and McTaggart-Cowan, R.: Tropical transition of Hurricane Chris (2012) over the North Atlantic Ocean: a multi-scale investigation of predictability, Monthly Weather Review, https://doi.org/10.1175/MWR-D-18-0188.1, 2019.

Marche Region Council Deliberation no. 148, Att. 1: La correlazione tra le allerte diramate e le conseguenti azioni operative, https://www.regione.marche.it/Portals/0/Protezione_Civile/Atti/DGR0148_18.pdf?ver=2018-02-26-165127-910&ver=2018-02-26-165127-910, (document in Italian), last access: 12 June 2020, 2018.

Mysiak, J., Testella, F., Bonaiuto, M., Carrus, G., De Dominicis, S., Ganucci Cancellieri, U., Firus, K., and Grifoni, P.: Flood risk management in Italy: challenges and opportunities for the implementation of the EU Floods Directive (2007/60/EC), Nat. Hazards Earth Syst. Sci., 13, 2883–2890, https://doi.org/10.5194/nhess-13-2883-2013, 2013.

MunichRe: Natural catastrophes 2017: https://www.munichre.com/content/dam/munichre/global/content-pieces/documents/TOPICS_GEO_2017-en.pdf, last access: 11 June 2020, 2018.

Nikolopoulos, E. I., Anagnostou, E. N., and Borga, M.: Using high-resolution satellite rainfall products to simulate major flash flood event in northern Italy, American Meteorological Society, 14, 171-185, doi: 10.1175/JHM-D-12-09.1; 2013.

Norbiato, D., Borga, M., and Dinale, R.: Flash flood warning in ungauged basins by use of the flash flood guidance and model-based runoff thresholds, Meteorol. Appl., 16, 65–75, https://doi.org/10.1002/met.126, 2009.

Patra, J. P., Kumar, R., and Mani, P.: Combined fluvial and pluvial flood inundation modelling for a project site, Procedia Technology, 24, 93-100, doi:10.1016/j.protcy.2016.05.014, 2016.

Rabiner, L. R. and Gold, B.: Theory and Application of Digital Signal Processing. Englewood Cliffs, NJ: Prentice-Hall, p. 401, ISBN 0139141014, 1975.

Rabiner, L.R. and Schafer, R.W.: Digital Processing of Speech Signals. Signal Processing Series. Upper Saddle River, NJ: Prentice Hall., 147–148, ISBN 0132136031, 1978.

Rabuffetti, D., Ravazzani, G., Corbari, C., and Mancini M.: Verification of operational Quantitative Discharge Forecast (QDF) for a regional warning system – the AMPHORE case studies in the upper Po River, Nat. Hazards Earth Syst. Sci., 8, 161–173, 2008.

Ranit, A. B. and Durge, P. V.: A review on different techniques of flood forecasting and their applications, International Journal of Advance Engineering and Research Development, 5, Issue 06, e-ISSN: 2348 - 4470, print-ISSN: 2348-6406, 2018.

Raynaud, D., Thielen, J., Salamon, P., Burek, P., Anquetin, S., and Alfieri, L.: A dynamic runoff coefficient to improve flash flood early warning in Europe: validation on the 2013 Central European floods in Germany, Meteorol. Appl., 22, 410–418, 2015.

Ravazzani, G., Gianoli, P., Meucci, S., and Mancini, M.: Assessing downstream impacts of detention basins in urbanized river basins using a distributed hydrological model, Water Resour Manag, 28(4), 1033–1044, doi:10.1007/s11269-014-0532-3, 2014.

Reed, S., Schaake, J., and Zhang, Z.: A distributed hydrologic model and threshold frequency-based method for flash flood forecasting at ungauged locations, Journal of Hydrology, 337, 402-420, 2007.

Rodda, J. C.: Guide to Hydrological Practices, Hydrological Sciences Journal, 56:1, 196-197, doi: 10.1080/02626667.2011.546602, 2011.

Salvati, P., Petrucci, O., Rossi, M., Bianchi, C., Pasqua, A. A., and Guzzetti, F.: Gender, age and circumstances analysis of flood and landslide fatalities in Italy, Science of The Total Environment, 610–611, 867-879, ISSN 0048-9697, https://doi.org/10.1016/j.scitotenv.2017.08.064, 2018.

Sangelantoni, L., Tomassetti, B., Colaiuda, V., Lombardi, A., Verdecchia, M., Ferretti, R., and Redaelli, G.: On the use of original and bias-corrected climate simulations in regional-scale hydrological scenarios in the Mediterranean basin, Atmosphere, 10, 799, https://doi.org/10.3390/atmos10120799, 2019.

Schroeder, A. J., Gourley, J .J., Hardy, J., Henderson, J.,J., Parhi, P., Rahmani,, V., Reed, K. A., Schumacher, R. S., Smith, B. K., and Taraldsen, M. J.: The development of a flash flood severity index, Journal of Hydrology, 541, 523-532, 2016.

Silvestro, F., Rebora, N., Giannoni, F., Cavallo, A., and Ferraris, L.: The flash flood of the Bisagno Creek on 9th October 2014: An "unfortunate" combination of spatial and temporal scales, Journal of Hydrology, 541, 50-62, Part A, ISSN0022-1694, https://doi.org/10.1016/j.jhydrol.2015.08.004, 2015.

Taraglio, S., Chiesa, S., La Porta, L., Pollino, M., Verdecchia, M., Tomassetti, B., Colaiuda, V., and Lombardi, A.: DSS for smart urban management: resilience against natural phenomena and aerial environmental assessment. International Journal of Sustainable Energy Planning and Management (forthcoming). doi:10.5278/ijsepm.3338, http://dx.doi.org/10.5278/ijsepm.3338, 2019.

Teng, J., Jakeman, A. J., Vaze, J., Croke, B. F. W., Dutta, D., and Kim, S.: Flood inundation modelling: A review of methods, recent advances and uncertainty analysis, Environmental Modelling & Software, 90, 201-216, 2017.

Tiber Basin Authority: Adozione del piano di gestione del distretto idrografico Appennino Centrale, Offical Bulletin of the Italia Republic, no. 72, Issued on 3 April 2010 (document in Italian), https://www.gazzettaufficiale.it/eli/gu/2010/04/03/78/sg/pdf , last access: 12 June 2020, 2010.

Tomassetti, B., Coppola, E., Verdecchia, M., and Visconti, G.: Coupling a distributed grid based hydrological model and MM5 meteorological model for flooding alert mapping, Adv Geosci, 2, 59–63, 2005.

Umbria Region Council Deliberation no. 2312/2007, Att. B: Procedure operative per la prima attuazione della Direttiva del Presidente del Consiglio dei Ministri del 27 febbraio 2004, Indirizzi operativi per la gestione organizzativa e funzionale del sistema di allertamento nazionale e regionale per il rischio idrogeologico e idraulico ai fini di protezione civile, http://www.regione.umbria.it/documents/18/211357/Direttiva+regionale+per+l%27allertamento+rischi+idrogeologico-+idraulico/d269c2e3-9372-4d43-8d2e-ce8babb00959, last access: 12 June 2020, 2007.

Verdecchia, M., Coppola, E., Faccani, C., Ferretti, R., Memmo, A., Montopoli, M., Rivolta, G., Paolucci, T., Picciotti, E., Santacasa, A., Tomassetti, B., Visconti, G., and Marzano, F. S.: Flood forecast in complex orography coupling distributed hydrometeorological models and in-situ and remote sensing data, Meteorol. Atmos. Phys., 101, 267–285, 2008a.

Verdecchia, M., Coppola, E., Tomassetti, B., and Visconti, G.: Cetemps Hydrological Model (CHyM), a Distributed Grid-Based Model Assimilating Different Rainfall Data Sources. In: Sorooshian S., Hsu KL., Coppola E., Tomassetti B., Verdecchia M., Visconti, G. (eds) Hydrological Modelling and the Water Cycle. Water Science and Technology Library, vol 63: 165-201. Springer, Berlin, Heidelberg, doi: 10.1007/978-3-540-77843-1_8, 2008b.

Vieux, B. E. and Bedient, P. B.: Assessing urban hydrologic prediction accuracy through event reconstruction, Journal of Hydrology, 299, 217-236, 2004.

Volpi, E., Di Lazzaro, M., Bertola, M., Viglione, A., and Fiori, A.: Reservoir effects on flood peak discharge at the catchment scale, Water Resources Research, 54, 9623–9636, 2018.

WMO: Guide to Hydrological Practices Volume II Management of Water Resources and Application of Hydrological Practices, ISBN 978-92-63-10168-6, 2009.

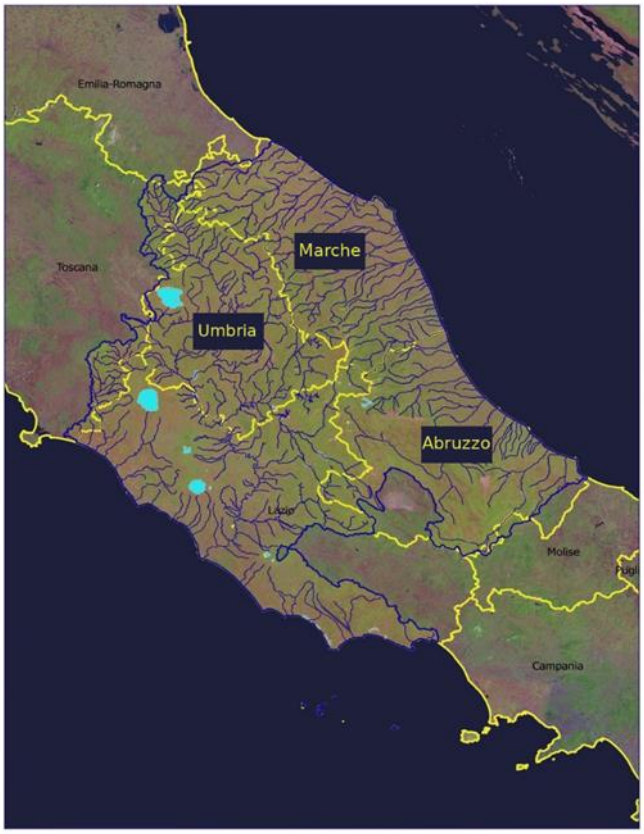

Figure 1: The Central Apennines Hydrological District (blue solid lines) and its main hydrography (blue thin lines). The north-eastern boundary is delimited by the Potenza river basin, while the south-eastern limit is represented by the Sangro basin in Abruzzo. The western side is delimited by the Tiber basin. Yellow lines indicate administrative boundaries of Italian regions. The three considered regions were highlighted: Umbria, Marche, Abruzzo (courtesy of Tiber Basin Authority, http://www.autoritadistrettoac.it/).

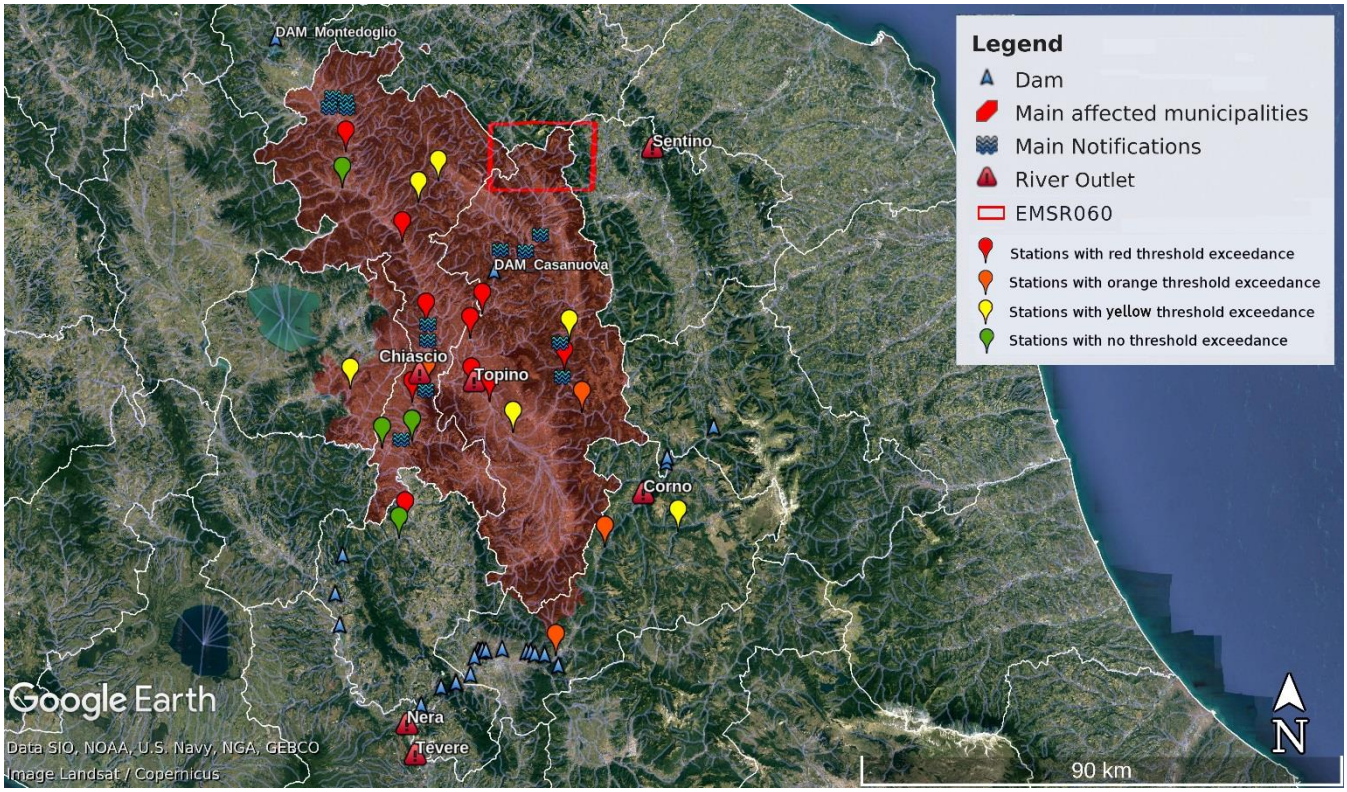

Figure 2: geo-referred information of ODB for CS01, Umbria Region, with localization of main recorded floods (blue waves), hydrometric stations used for the indices validation (pinpoints). Red triangles indicate the position of outlets of main involved rivers, while blue triangles indicate the presence of dams. Hydrometric station pinpoints are coloured according to the maximum hydrometric threshold reached during the event. Municipalities areas affected by floodings are filled in red. Red rectangle represents the involved area published on COPERNICUS Emergency Management Service Platform (https://emergency.copernicus.eu/mapping/list-of-components/EMSR060). ©Google Earth

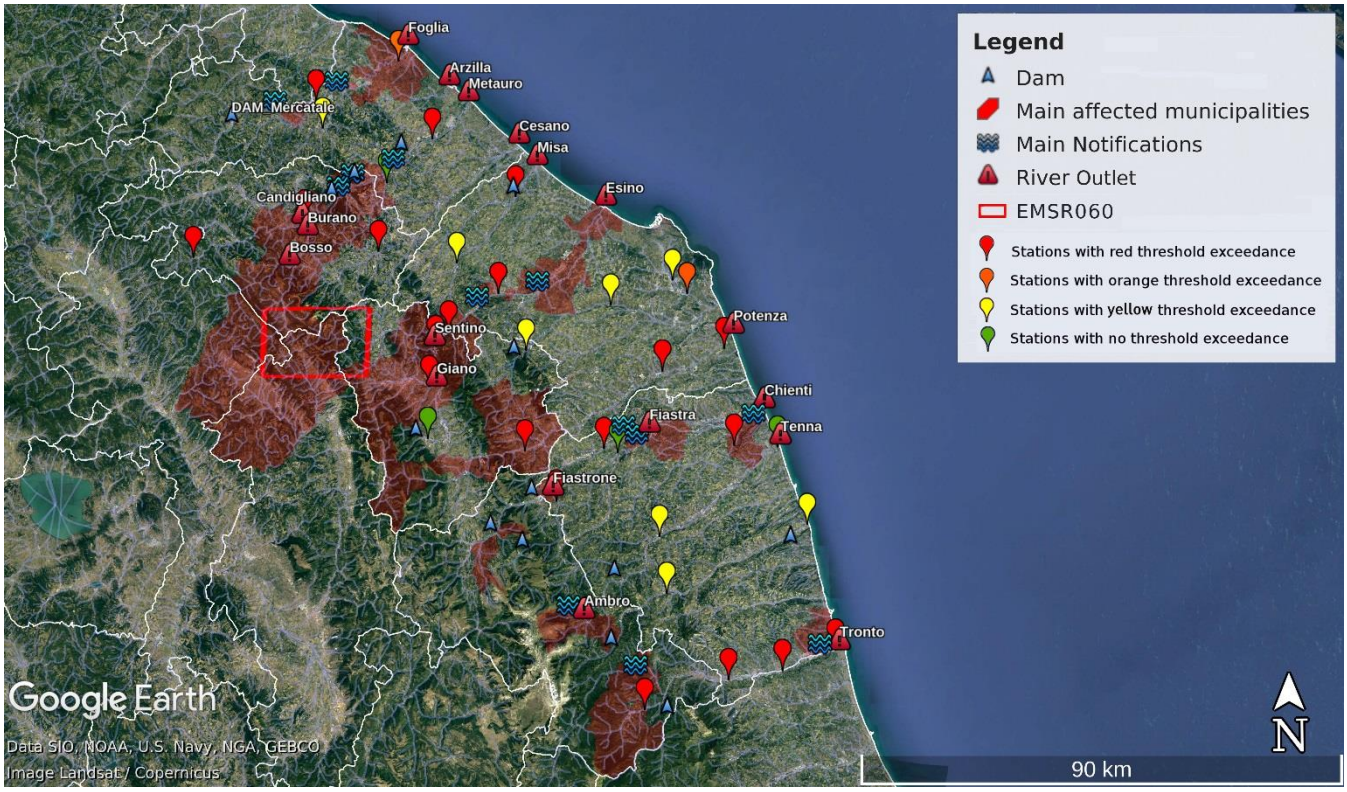

Figure 3: geo-referred information of ODB for CS02, Marche Region, with localization of main recorded floods (blue waves), hydrometric stations used for the indices validation (pinpoints). Red triangles indicate the position of outlets of main involved rivers, while blue triangles indicate the presence of dams. Hydrometric station pinpoints are coloured according to the maximum hydrometric threshold reached during the event. Municipalities areas affected by floodings are filled in red. ©Google Earth

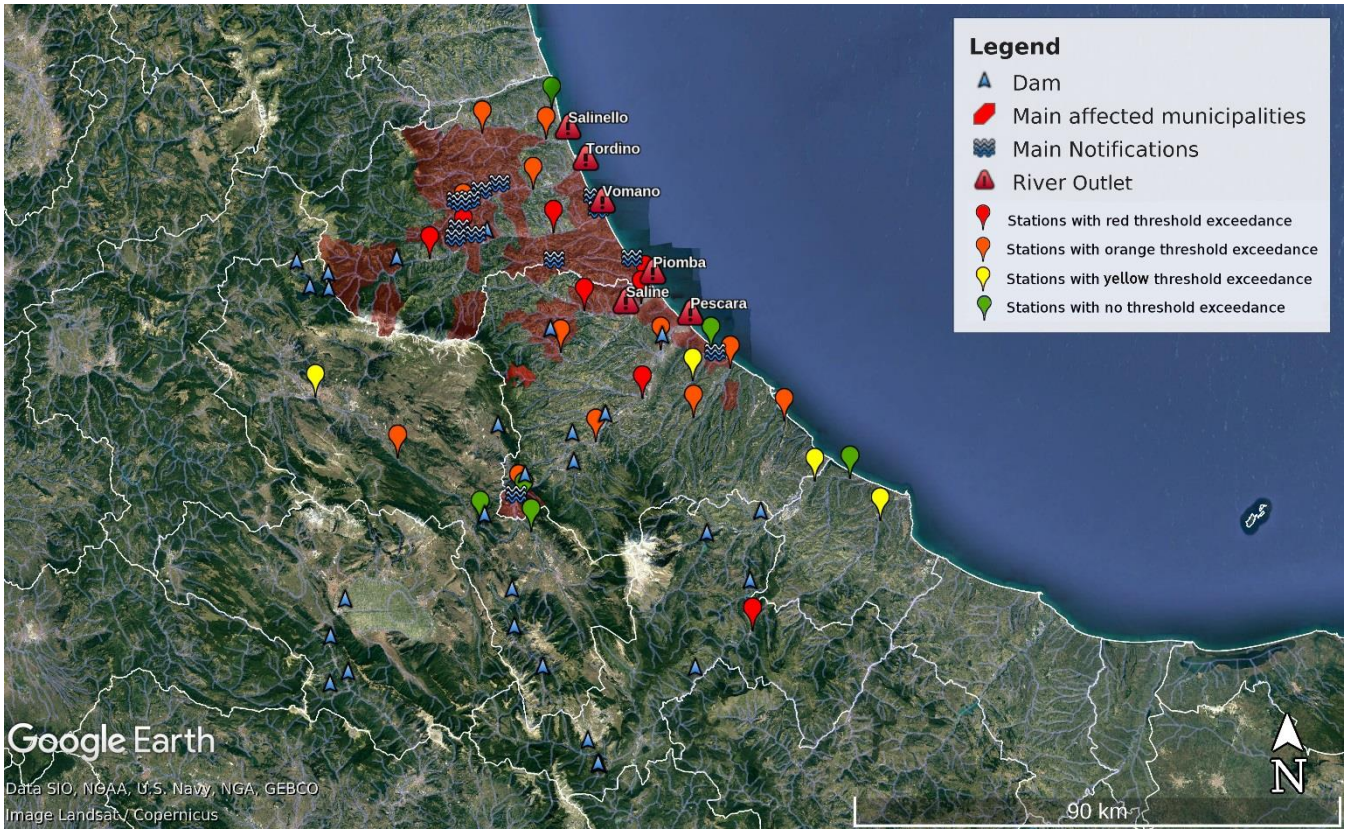

970

Figure 4: geo-referred information of ODB for CS03, Abruzzo Region, with localization of main recorded floods (blue waves), hydrometric stations used for the indices validation (pinpoints). Red triangles indicate the position of outlets of main involved rivers, while blue triangles indicate the presence of dams. Hydrometric station pinpoints are coloured according to the maximum hydrometric threshold reached during the event. Municipalities areas affected by floodings are filled in red. ©Google Earth

975

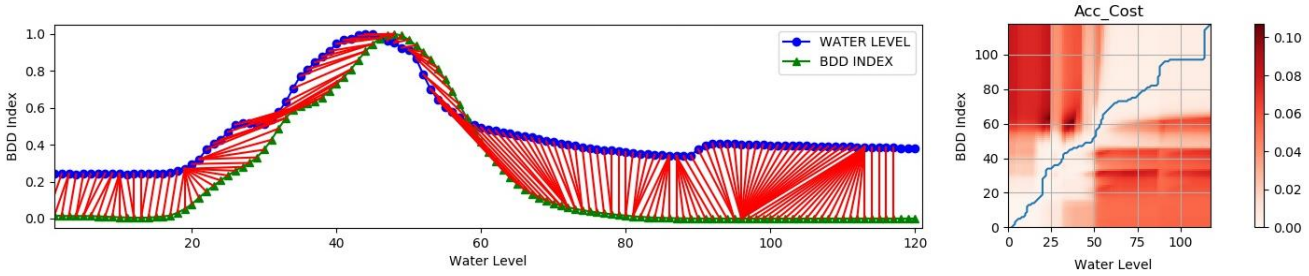

Figure 5: graphical representation of DDTW correspondences between two first derivatives of time series x(t) and y(t). In this case, time series are represented by two generic profiles of the hydrometric water level and the BDD index, at the same station point (from Keogh and Pazzani, 2001).

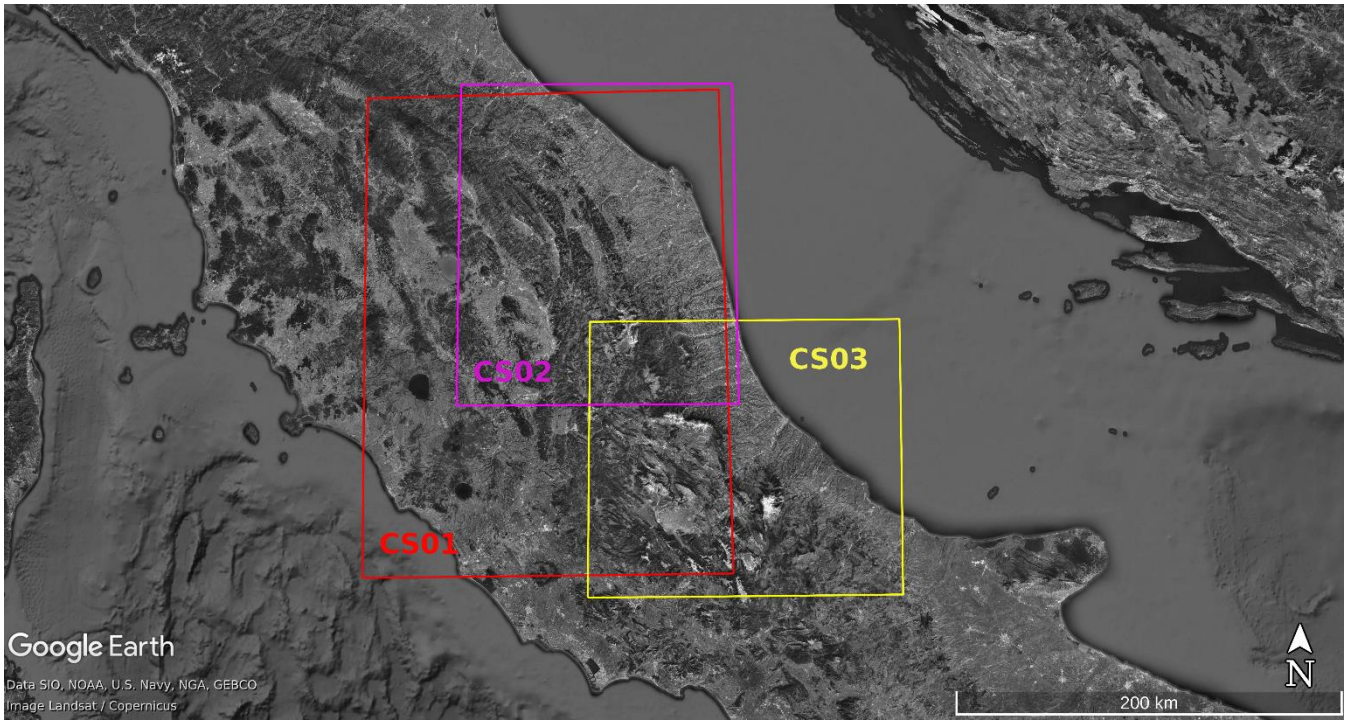

Figure 6: three CHyM geographical domains used for the simulation of the corresponding CSs. The red square encloses Umbria Region and the rest of Tiber basin for CS01, pink square refers to CS02 (Marche Region) and yellow square encompasses Abruzzo Region for CS03. ©Google Earth

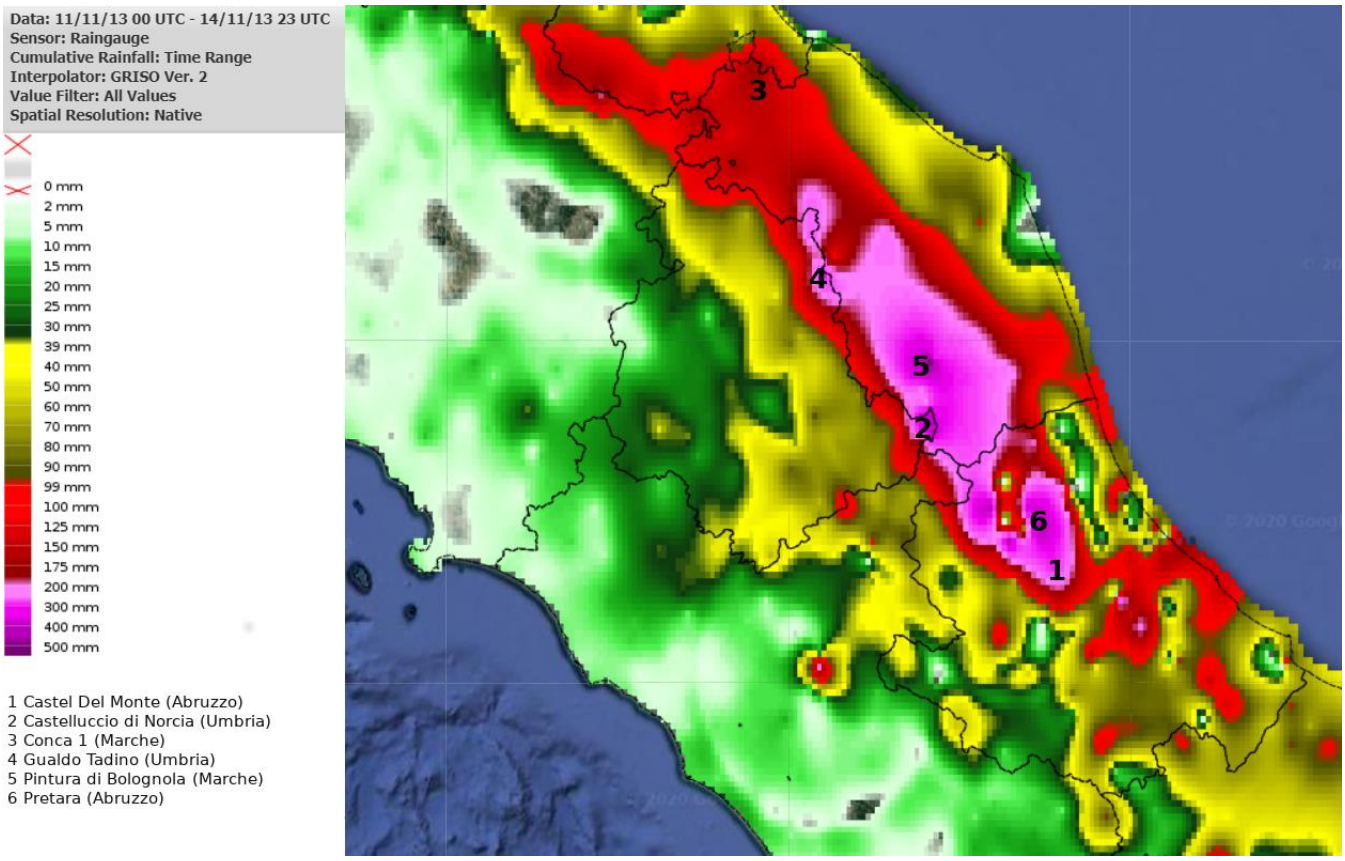

Figure 7: total accumulated rainfall (spatialization from rain gauges official network) during the event, from 11st November 2012 00 UTC to 13rd November 2013, 23 UTC (picture generated from the Dewetra Platform, Italian Civil Protection Department and CIMA Research Foundation, 2014). The localization of the six raingauges were indicated on the map: 1) Castel del Monte station (Abruzzo Region), 2) Castelluccio di Norcia station (Umbria Region), 3) Conca 1 station (Marche Region), 4) Gualdo Tadino station (Umbria Region), 5) Pintura di Bolognola station (Marche Region); 6) Pretara station (Abruzzo Region). The raingauges recorded significant accumulated rain (up to 400 mm per 72 hours, purple area).

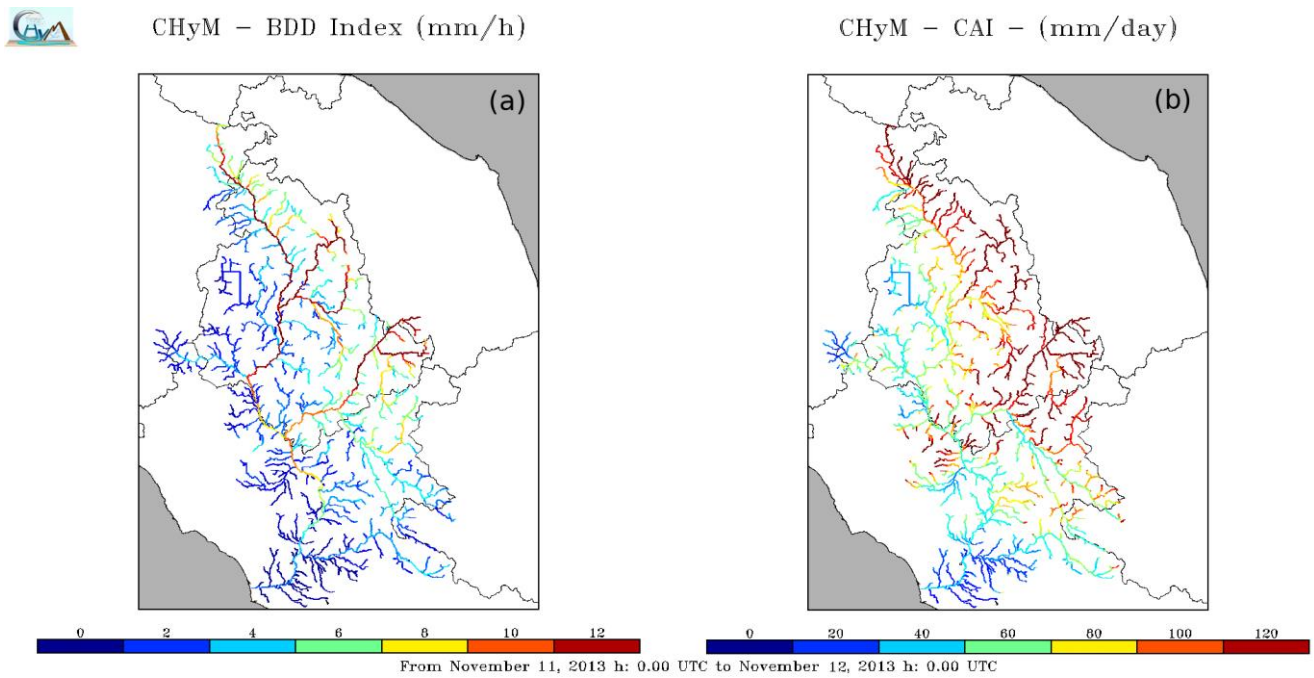

Figure 8: CS01 24 hours maps of BDD index (left) and CAI index (right) obtained for November 11th, 2013, by forcing the CHyM model with observed rainfall data. Warmer colours indicate river segments with higher flood stress. In both figures, the Umbria region drainage network, as well as the whole Tiber river basin, are highlighted.

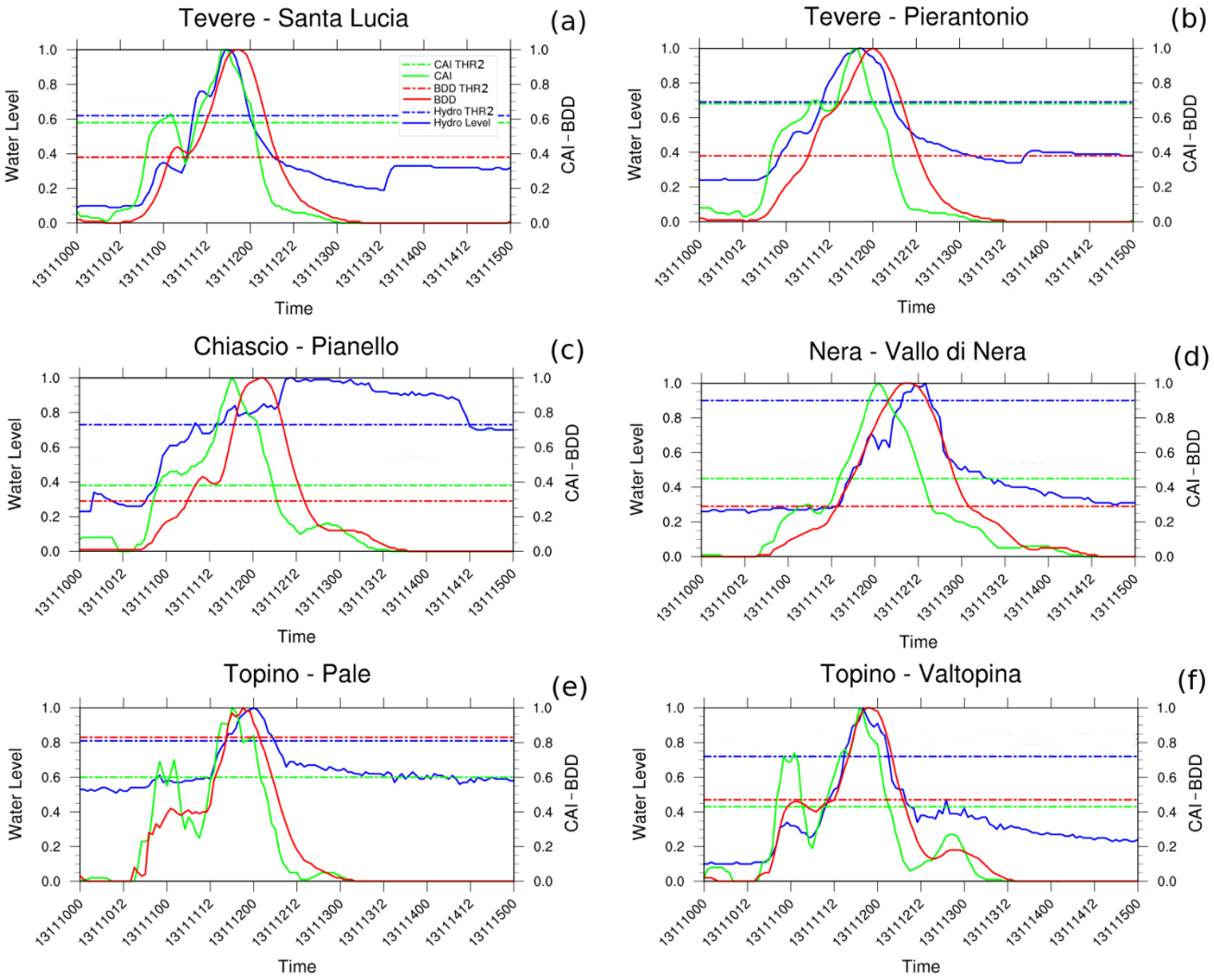

1005

Figure 9: time series comparison for six hydrometric stations: BDD hourly profile (red line), BDD Moderate Threshold (red flat line); CAI hourly profile (green line), CAI Moderate Threshold (green flat line); Hydrometric Level hourly profile (blue line), Hydrometric Level Moderate Threshold (blue flat line). Quantities profiles and related thresholds are normalized.

1010

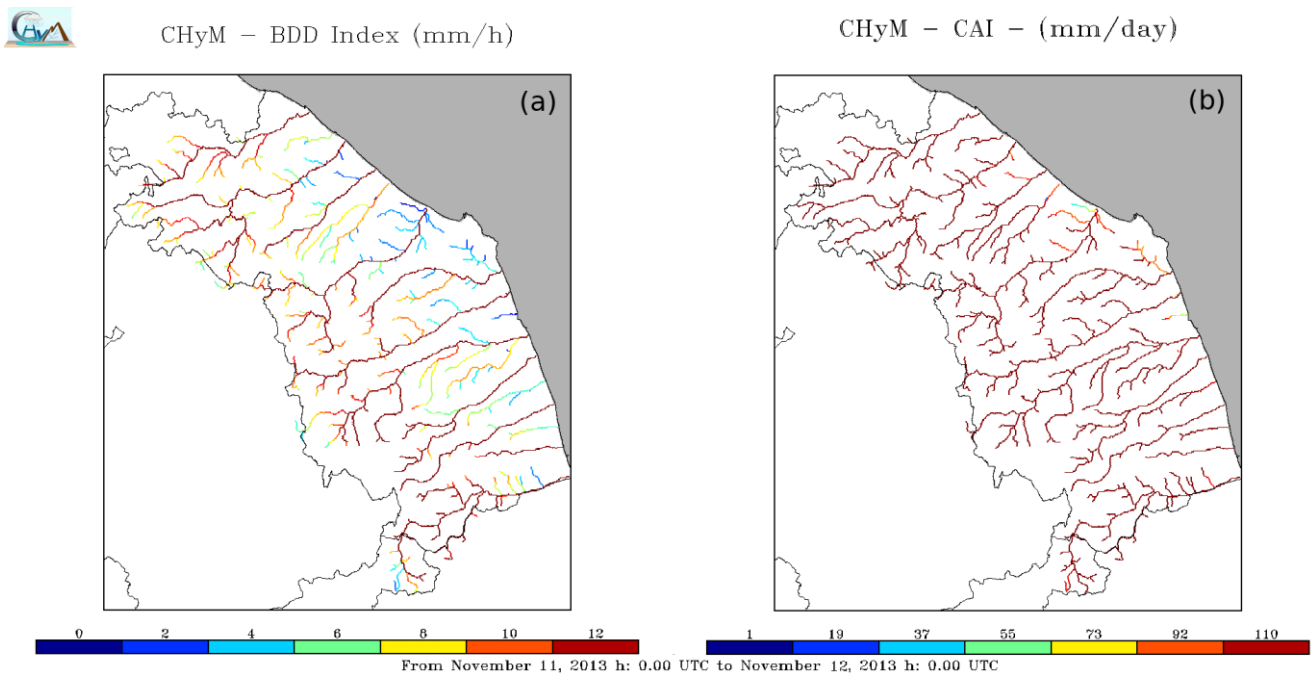

Figure 10: CS02 24 hours maps of BDD index (left) and CAI index (right) obtained for November 11th 2013, by forcing the CHyM model with observed rainfall data. Warmer colours indicate river segments with higher flood stress. In both figures, the Marche region drainage network is highlighted.

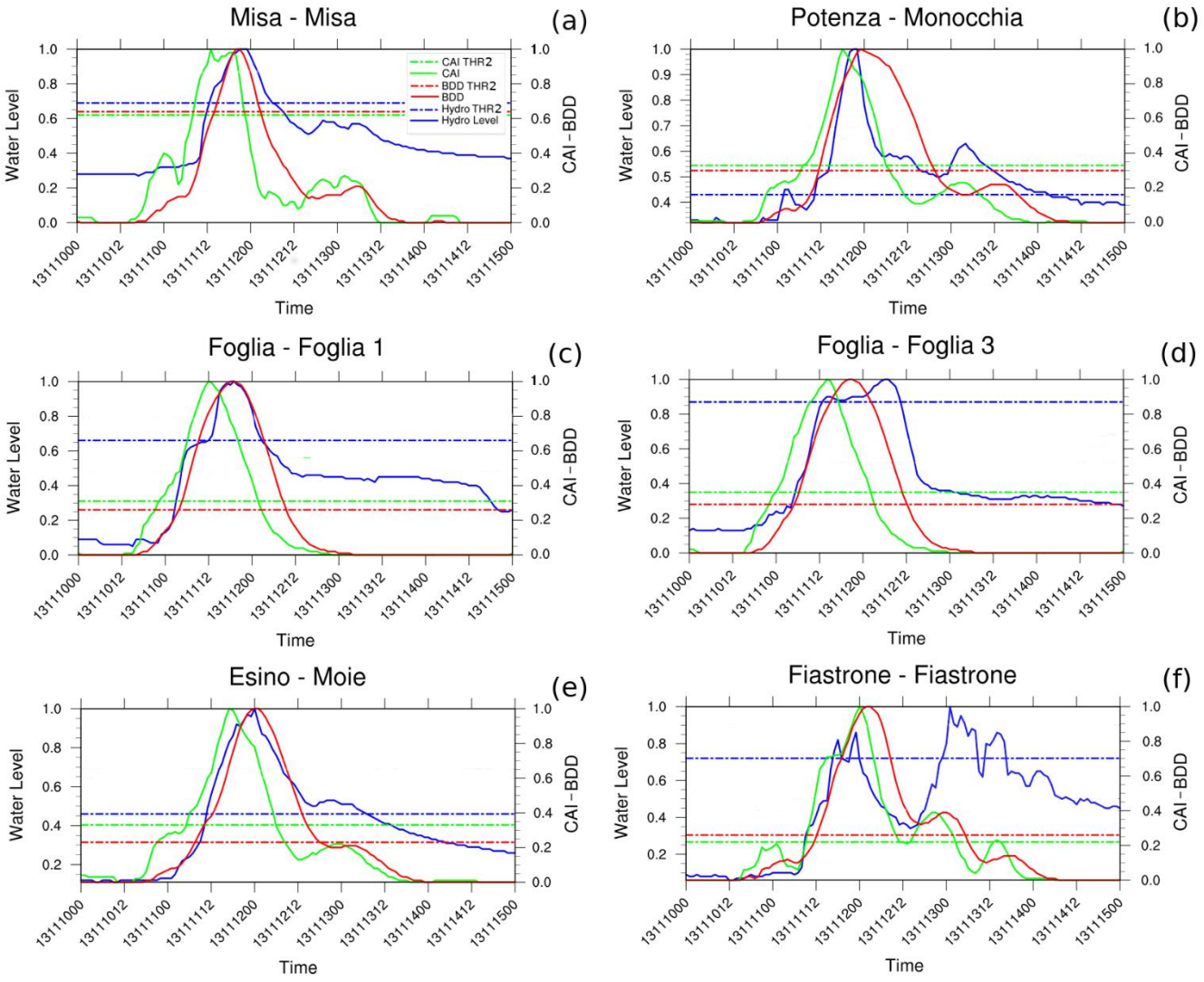

Figure 11: time series comparison for six hydrometric stations: BDD hourly profile (red line), BDD Moderate Threshold (red flat line); CAI hourly profile (green line), CAI Moderate Threshold (green flat line); Hydrometric Level hourly profile (blue line), Hydrometric Level Moderate Threshold (blue flat line). Quantities profiles and related thresholds are normalized.

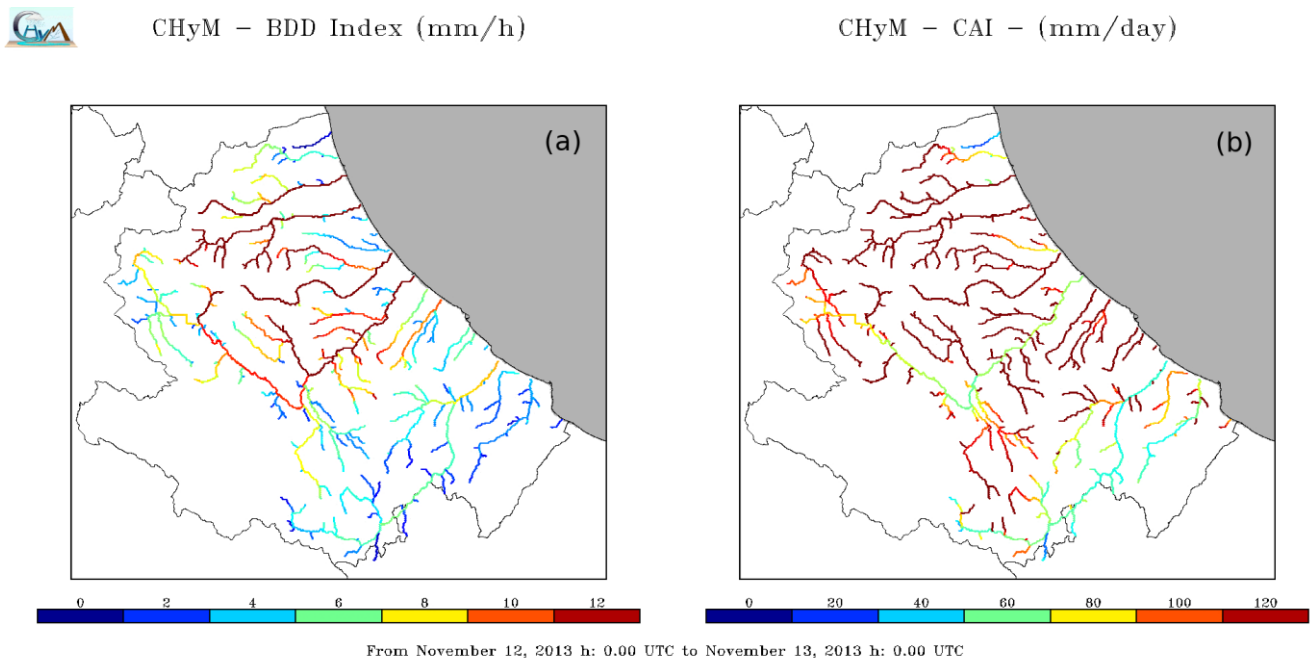

Figure 12: CS03 24 hours maps of BDD index (left) and CAI index (right) obtained for November 12th 2013, by forcing the CHyM model with observed rainfall data. Warmer colours indicate river segments with higher flood stress. In both figures, the Abruzzo region drainage network, belonging to the Central Apennine District, is highlighted

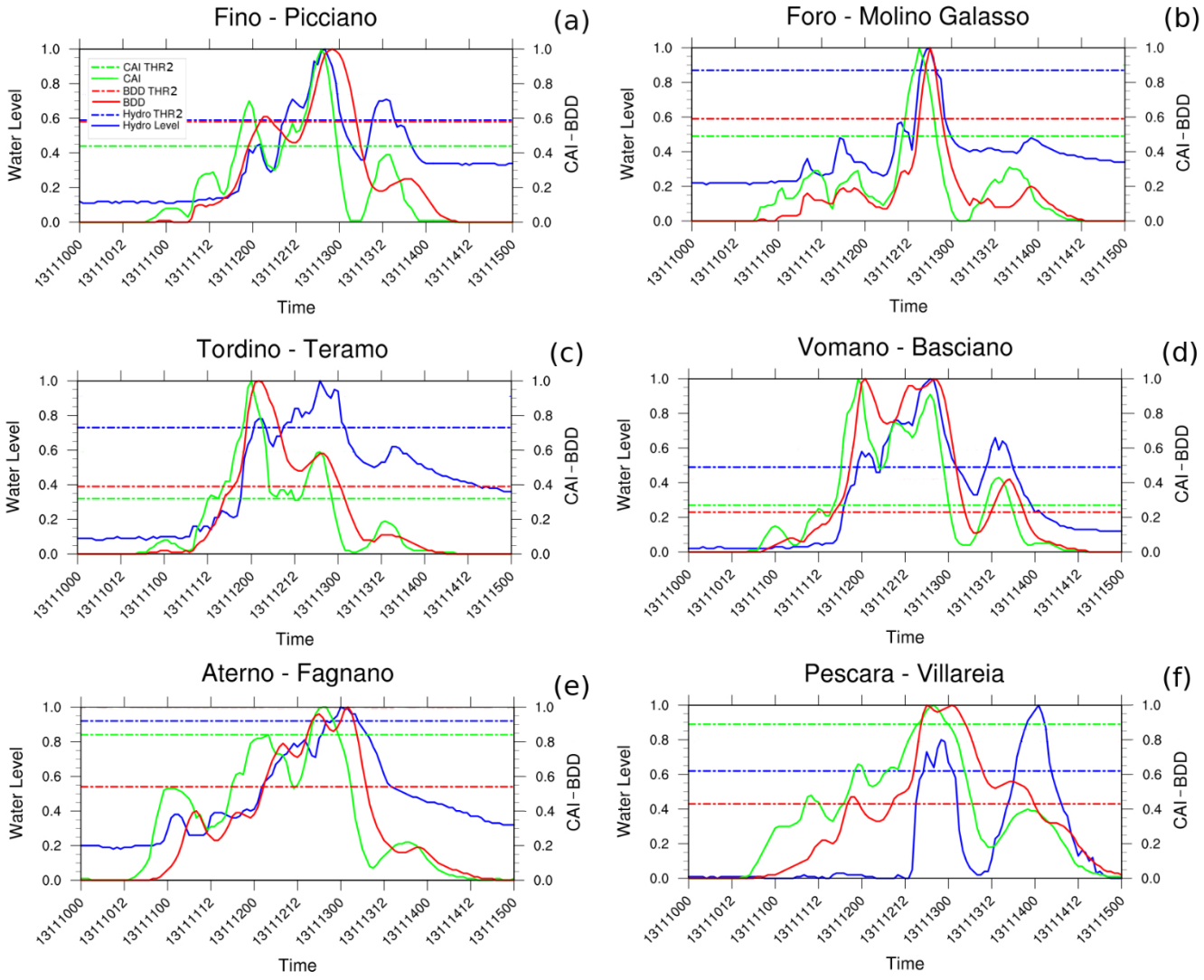

1035 **Figure 13**: time series comparison for six hydrometric stations: BDD hourly profile (red line), BDD Moderate Threshold (red flat line); CAI hourly profile (green line), CAI Moderate Threshold (green flat line); Hydrometric Level hourly profile (blue line), Hydrometric Level Moderate Threshold (blue flat line). Quantities profiles and related thresholds are normalized.

.

1040

Table 1: hydrogeological criticality levels officially defined by the Civil Protection Authorities. Regional Functional Centres define hydrometric thresholds, in relevant river sections. Those thresholds are based on the return period concept, in order to individuate the ciricality level to be assigned to the whole warning area (definitions conformed to Deliberation of Abruzzo Region Council no.659/2017, Deliberation of Marche Region Council no. 148/2018 and Deliberation of Umbria Region Council no. 2312/2007).

Threshold Colour-code	Hydrometric level	Criticality level	Description
Green	Below THR1	Absence of significant predictable phenomena	Regular Criticality Level, possible local floods due to non-sufficient drainage of meteoric waters
Yellow	Above THR1 (Yellow threshold)	Ordinary Criticality	Ordinary Criticality Level: Weak flow peak. Water level values corresponds to low water level and generally below the natural terrain level.
Orange	Above THR2 (Orange threshold)	Moderate Criticality	Moderate Criticality Level. Flow peak with limited erosion and transport. Water levels corresponds to the floodplain and river expansion to the levee. The natural floodplain is exceeded.
Red	Above THR3 (Red Threshold)	High criticality	High Criticality Level. Significant discharge peak and diffused erosion and transport. Water Level corresponds to the whole riverbed.

Table 2: summary of relevant damages reported for each Case Study and used information sources.

Case Study	Date	Region	Reported damages	Information sources		
				OR	PR	V
CS01	11-12 Nov 2013	Umbria	Interruption of several roads and bridges, isolated villages, damage to buildings and roads, a hospital isolated. ***Important notes from OR*** The large dams in the Tiber basin (Montedoglio and Corbara on Tiber and Casanuova on Chiascio river) played a crucial role for the storage of upstream incoming volumes, allowing the lamination and the misalignment of the full floods downstream.	✓	✓	✓
CS02	11-12 Nov 2013	Marche	Interruption of several roads, houses evacuated, isolated villages and two fatalities. ***Important notes from OR*** The large dams in the Foglia, Metauro, Chienti and Tronto basins played a crucial role for the storage of upstream incoming volumes and allowed the lamination and the misalignment of the full floods downstream.	✓	✓	✓
CS03	12-13 Nov 2013	Abruzzo	Flooding phenomena affected the small Abruzzo Rivers. Interruption of several roads, damage to buildings and roads.	X	✓	✓
Legend: OR: Official Civil Protection Report; **PR:** Press releases; **V:** Videos						

Table 3: contingency table structure used for the validation analysis.

		Observed	
		Yes	No
Estimated	Yes	Hit (H)	False Alarm (FA)
	No	Miss (M)	Correct Negative (CN)

Table 4: CHyM domain set-up for the analysed case studies. Please, note that the rain gauges data may not be all available during the entire event, due to interruption of electric supply.

	CS01	**CS02**	**CS03**
Horizontal Resolution	370 m	270 m	270 m
Domain dimension (nlon*nlat)	750x550	650x550	710x470
No. of hourly timesteps	240	240	240
No. of rain gauges in the domain	Up to 371	Up to 138	Up to 135
No. of hydrometric stations used in the domain	22	28	26

Table 5: CAI and BDD indices scores for all CSs. Values for single CS are averages calculated over all hydrometric stations located in the domain.

BDD								
	CR	**A**	**POD**	**FAR**	**LTP**	**RLTP**	**CTD**	**DDTW**
CS01	0.86	0.88	0.70	0.46	-0.6	-0.05	-1.0	0.02
CS02	0.75	0.85	0.68	0.37	0.4	0.04	-1.4	0.04
CS03	0.77	0.91	0.80	0.48	-8.6	-1.11	-4.2	0.09
TOT	**0.79**	**0.88**	**0.72**	**0.43**	**-2.9**	**-0.37**	**-2.2**	**0.05**
CAI								
	CR	**A**	**POD**	**FAR**	**LTP**	**RLTP**	**CTD**	**DDTW**
CS01	0.77	0.88	0.51	0.44	-8.5	-0.67	-7.4	0.06
CS02	0.75	0.82	0.55	0.43	-4.8	-0.56	-5.6	0.05
CS03	0.77	0.93	0.72	0.40	-12.6	-1.59	-7.62	0.11
TOT	**0.76**	**0.88**	**0.59**	**0.42**	**-8.6**	**-0.94**	**-6.9**	**0.07**